



Descriptions of neurocranium morphology in 34 species of moray eels (Muraenidae) found in Taiwan

MARITES RAMOS-CASTRO¹, HONG-MING CHEN^{1,2,3} & BO-SYUN MAO¹

¹Department of Aquaculture, College of Life Sciences, National Taiwan Ocean University, Keelung, 20224, Taiwan

²Center of Excellence for the Oceans, National Taiwan Ocean University, Keelung, 20224, Taiwan

¹ maritescastro22@yahoo.com; <https://orcid.org/0000-0002-4265-3865>

^{1,2,3} hmchen@mail.ntou.edu.tw; <https://orcid.org/0000-0002-3921-2022>

¹ M97330046@mail.ntou.edu.tw; <https://orcid.org/0000-0002-0506-982X>

³Corresponding author

Abstract

Taiwan is one of the richest in the world in terms of eel fauna. In this study, we examined the osteological and morphological characteristics of eels in the family Muraenidae. Furthermore, we focused on the neurocranium of 34 muraenid species in the genera *Echidna* (2), *Enchelycore* (3), *Gymnomuraena* (1), *Gymnothorax* (25), *Scuticaria* (1), *Strophidon* (1), and *Uropterygius* (1), which are caught in Taiwanese waters. This paper shows the results of a comparative study on osteological characters of the neurocranium including the ratio of nine length characters and 20 diagnostic characters for 34 eel species in the family Muraenidae. The subfamily Uropterygiinae is distinguished from the subfamily Muraeninae in having the lowest value on the depth of mid pre-orbit due to the termination of the ethmoidal crest toward premaxilla. Moreover, aside from *Gymnomuraena zebra*, the species of subfamily Uropterygiinae have the lowest orbit length. These results in neurocranial comparative morphology between the species are consistent with their previous classification based on molecular results. These morphological and osteological characters may be valuable for taxonomic purposes and might be used as the basis for further studies on the status of genera in Muraenidae.

Key words: moray eels, morphology, Muraenidae, neurocranium, osteology

Introduction

Family Muraenidae is composed of 16 genera and 217 recognized species (Fricke *et al.*, 2020) and is a diverse family of eels found around the world (Smith, 2012). The family Muraenidae is one of the most abundant and widespread of all eel families. More than 40 species of the family Muraenidae are found in Taiwanese waters (Chen *et al.*, 1994; Shao *et al.*, 2008; Loh *et al.*, 2011).

Several classifications of moray eels used morphological characters to distinguish species. Past studies date back to 1989 (Böhlke *et al.*, 1989), when the neurocranium of *Muraena helena* was described. Of the skeletal structure, there was more emphasis on the number of vertebrae, dentition and external morphology as a basis for classification. Some scholars have also compared the skeletal structures of the pectoral girdle (Fielitz, 2002), cranial musculoskeletal anatomy (Reece *et al.*, 2010; Collar *et al.*, 2014), feeding mechanisms (Mehta & Wainwright, 2007), and implications of jaw elongation on the feeding apparatus in Nettastomatidae (Eagderi & Adriaens, 2014). Furthermore, major criteria in identification of moray eels include ratios of morphological measurements (Loh *et al.*, 2008), coloration patterns (Huang *et al.*, 2019), variegated markings, and dentition (Smith & Böhlke, 1997; Loh *et al.*, 2008).

In this present paper, we report on a comparative study of the neurocranium of 34 eel species in family Muraenidae. Many species were not thoroughly assessed at the intraspecific level, and there is little to no control for the ontogenetic stage of specimens across species. Our aim is to evaluate the relationship within moray eels found in Taiwan by neurocranium morphological comparison methods. Although the number of specimens and species is not enough to clarify all of the relationships, these data can serve as a basis for future investigation of cranial morphometrics in morays.

Materials and methods

Collecting and recording of samples

The specimens of moray eel were mainly caught by long-lines by the fishermen of Hualien and Taitung counties in eastern Taiwan, in 2000–2019, and the others were bought from Keelung Fish Market. A total of 72 specimens, representing 34 moray eel species from six genera under family Muraenidae, have been examined (Table 1).

Specimens were individually photographed and their measurements were recorded following Böhlke *et al.* (1989). Total lengths were recorded to the nearest one-tenth of a centimeter (0.1 cm). Specimens were registered and assigned a catalog number to the collections of the Laboratory of Aquatic Ecology, Department of Aquaculture, National Taiwan Ocean University (TOU-AE).

Production of skeletal specimens

The head of each specimen was boiled for three to five minutes, depending on size. The skin and flesh were gently removed using tweezers. The remaining flesh attached to the bones was softened by soaking in 1% NaOH solution for 20 to 30 minutes and was totally cleaned by brushing with a toothbrush. The eel skeletons were then air-dried for 24 hours.

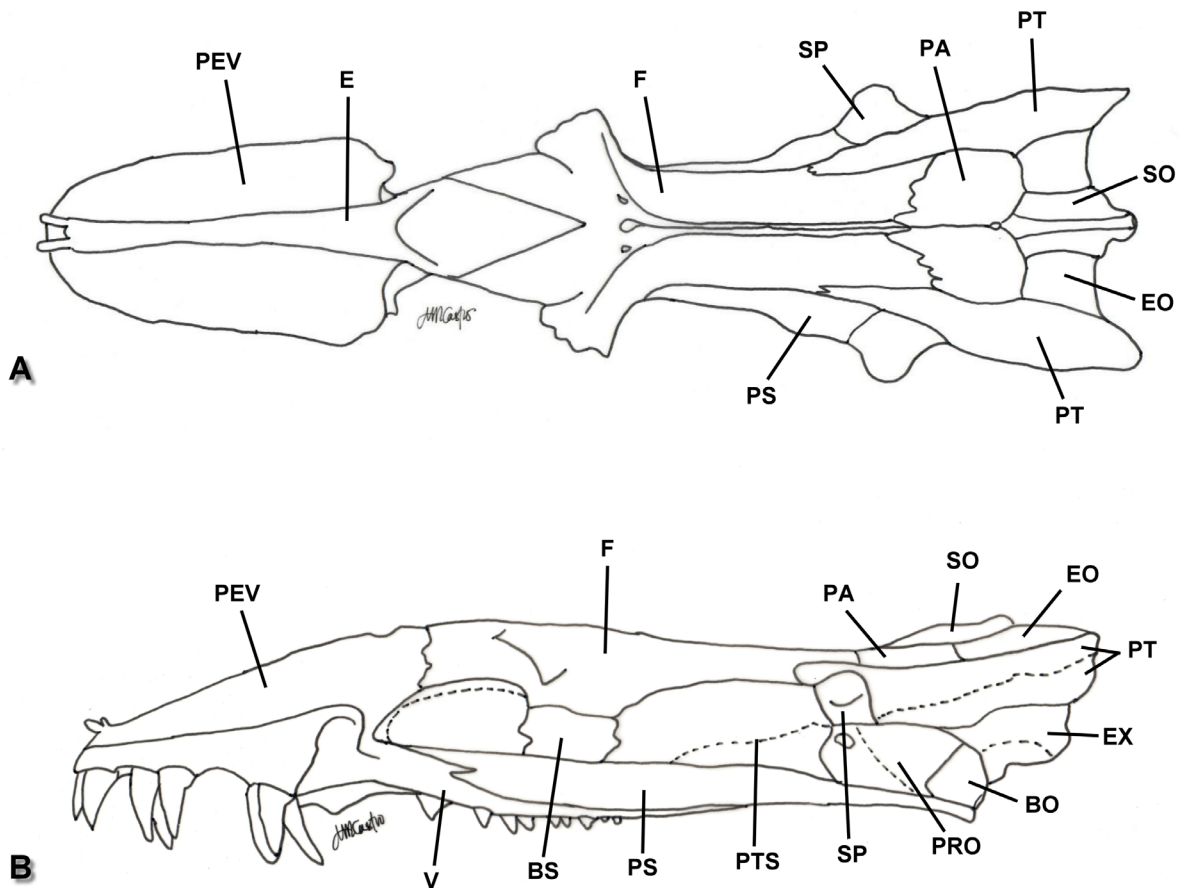


FIGURE 1. The name and abbreviation of the cranial skeletal elements. A. Dorsal view. B. Left lateral view. Abbreviations: BO: basioccipital; BS: basisphenoid; E: ethmoid; EX: exoccipital; EO: epiotic; F: frontal; P: premaxilla; PA: parietal; PAS: parasphenoid; PEV: premaxillary-ethmovomer; PRO: prootic; PT: pterotic; PTS: pterosphenoid; SO: supraoccipital; SP: sphenotic; V: vomer

TABLE 1. Neurocranium comparison from the average ratios of length measurements in 34 moray eel species.

Species	NCL/	NCL/	NCL/	NCL/	NCL/	NCL/	NCL/	NCL/
	NCW	EML	OBL	POBL	MPEVW	MFW	NCDB	mPOBD
<i>Echidna nebulosa</i>	3.37	2.25	6.58	3.99	5.78	6.10	4.80	7.39
<i>Echidna polyzona</i>	4.26	2.22	6.52	4.37	6.60	6.15	4.23	8.02
<i>Enchelycore lichenosa</i>	4.26	1.88	6.39	3.15	5.48	4.16	6.04	11.81
<i>Enchelycore pardalis</i>	3.89	1.92	5.60	2.92	6.65	5.59	5.06	11.92
<i>Enchelycore schismatorhynchus</i>	3.28	1.66	5.44	2.68	5.04	3.52	4.71	7.02
<i>Gymnomuraena zebra</i>	4.54	2.79	10.88	5.45	7.01	9.76	5.52	10.37
<i>Gymnothorax albimarginatus</i>	3.10	1.99	5.10	2.97	3.38	3.23	4.18	8.99
<i>Gymnothorax berndti</i>	3.82	1.92	5.67	3.23	5.97	5.16	5.43	7.55
<i>Gymnothorax buroensis</i>	3.18	1.94	5.84	3.81	4.67	3.87	4.10	6.82
<i>Gymnothorax chilospilus</i>	3.72	1.87	6.60	3.22	4.85	4.44	5.08	6.51
<i>Gymnothorax eurostus</i>	3.08	1.82	5.66	3.44	4.32	3.60	4.49	7.04
<i>Gymnothorax favagineus</i>	3.52	2.05	6.80	3.99	5.48	3.86	5.05	7.88
<i>Gymnothorax fimbriatus</i>	3.66	1.90	5.23	3.27	6.00	4.60	5.04	9.13
<i>Gymnothorax flavimarginatus</i>	3.58	2.03	6.51	4.16	5.17	3.88	4.51	5.59
<i>Gymnothorax formosus</i>	2.98	2.05	5.64	3.99	4.54	4.30	4.54	8.24
<i>Gymnothorax intesi</i>	3.78	2.17	5.93	3.93	5.53	4.99	5.27	9.43
<i>Gymnothorax kidako</i>	3.50	1.78	6.31	3.11	5.14	4.58	5.22	9.12
<i>Gymnothorax leucostigma</i>	3.98	1.74	5.40	3.76	5.08	5.04	5.17	8.04
<i>Gymnothorax margaritophorus</i>	3.82	1.82	6.09	2.97	5.97	5.26	4.78	7.89
<i>Gymnothorax meleagris</i>	3.50	1.94	5.78	3.83	4.72	3.76	4.73	8.35
<i>Gymnothorax minor</i>	3.59	2.14	5.59	3.16	5.19	4.06	5.07	8.13
<i>Gymnothorax monochrous</i>	3.22	2.03	6.13	3.36	4.81	4.53	3.70	6.48
<i>Gymnothorax mucifer</i>	3.72	1.86	5.85	3.17	5.63	5.24	5.17	8.45
<i>Gymnothorax neglectus</i>	3.94	1.87	6.13	3.08	6.01	5.14	5.03	9.98
<i>Gymnothorax nudivomer</i>	3.80	2.05	5.46	5.80	7.63	4.52	3.42	4.59
<i>Gymnothorax pictus</i>	3.72	1.99	5.20	3.55	5.15	4.38	4.52	6.96
<i>Gymnothorax pseudothyrsoides</i>	3.41	1.97	5.50	3.66	4.80	3.70	4.60	7.39
<i>Gymnothorax reevesii</i>	3.54	2.02	5.77	3.51	3.97	3.32	4.16	8.21
<i>Gymnothorax thyrsoides</i>	3.50	2.11	6.53	3.91	4.96	5.03	4.21	6.74
<i>Gymnothorax undulatus</i>	3.90	2.04	5.93	2.78	6.01	4.94	5.28	10.53
<i>Gymnothorax ypsilon</i>	3.84	1.83	5.68	2.96	6.46	5.52	5.71	9.76
<i>Scuticaria tigrina</i>	3.39	2.17	7.06	3.75	4.45	4.93	5.59	14.75
<i>Strophidon sathete</i>	3.16	2.05	6.20	4.01	4.56	4.23	5.15	6.63
<i>Uropterygius macrocephalus</i>	3.47	1.91	7.12	3.05	6.00	4.98	4.23	19.82

The cranial and skeletal regions were compared according to Böhlke *et al.* (1989). The bony elements (Fig. 1) were also identified as below:

- Basioccipital (BO): at the end of the occipital base.

- Basisphenoid (BS): at the back of the orbital.
- Ethmoid (E): median wall before the orbit and anterodorsal part of neurocranium.
- Epiotic (EO): upper element of pterotic.
- Exoccipital (EX): bone connected to the wing below pterotic
- Frontal (F): paired epidermal bones at the top of the skull above the eye, paired and separated by a ridge.
- Parasphenoid (PS): median and elongated bone situated at the base of the neurocranium
- Parietal (PA): between the frontals and the upper occipital, often a pair.
- Premaxillary-ethmovomer (PEV): premaxilla connecting to the ethmoid and vomer plate.
- Prootic (PRO): site of the socket of hyomandibular attachment and situated lateroventrally under the sphenotic.
- Pterotic (PT): lower part of epiotic that expands laterally and protrudes posteriorly.
- Pterosphenoid (PTS): bone connected to the base of the sphenotic.
- Sphenotic (SP): small paired bone attached to the outer surface of the pterosphenoid.
- Supraoccipital (SO): central bone on posterodorsal part of neurocranium.

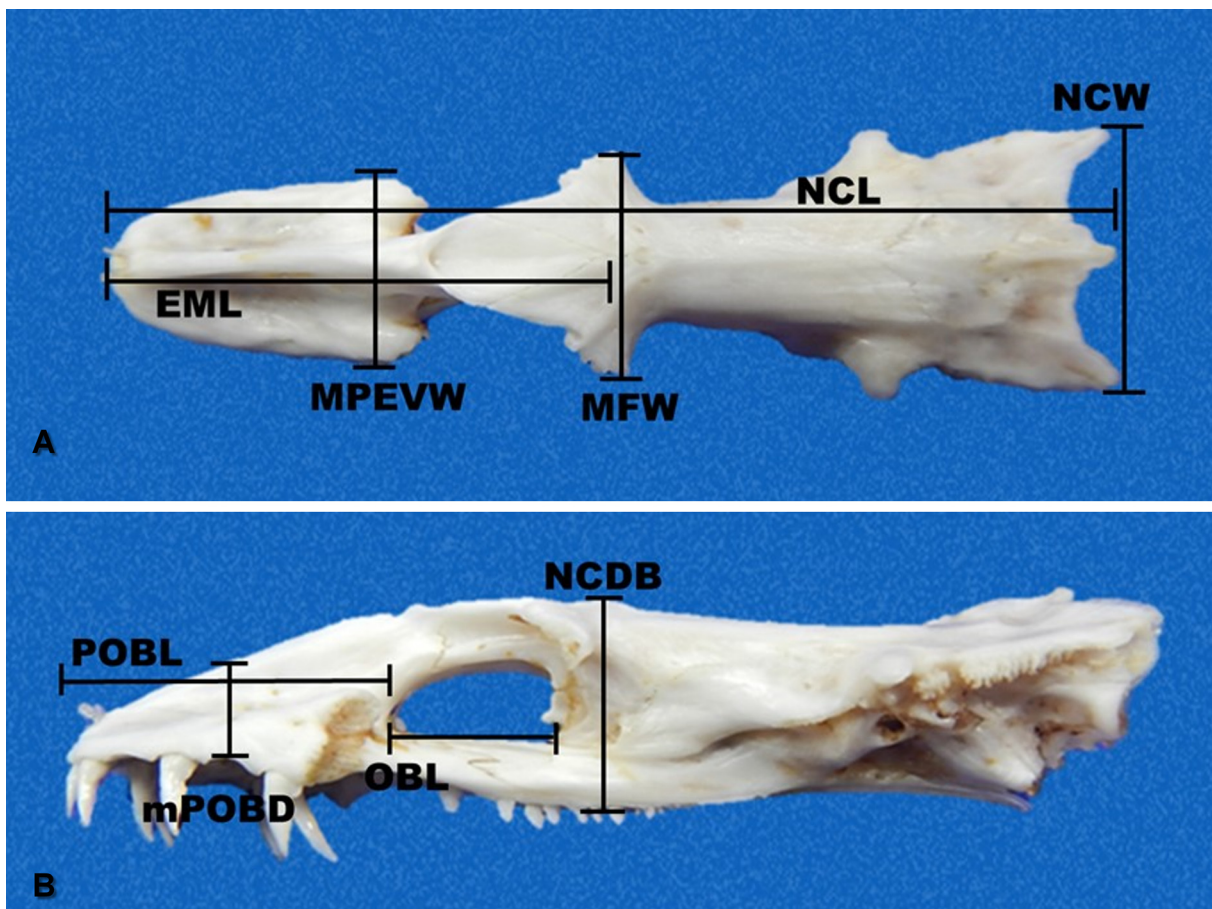


FIGURE 2. A. Dorsal and B. Left lateral view of *Gymnothorax kidako*, TOU-AE 7576, 71.0 cm TL. Location of cranial measurements including neurocranium length (NCL), neurocranium width (NCW), ethmoid length (EML), orbital length (OBL), pre-orbital length (POBL), maximum premaxillary-ethmovomer width (MPEV), maximum frontal width (MFW), neurocranium depth at basisphenoid (NCDB), and mid pre-orbital depth (mPOBD).

Definition of length measurements and ratios

Each neurocranium was photographed and measured to facilitate the comparison based on the length ratio and morphology. The measurements (Fig. 2) include neurocranium length (NCL), the distance between the anterior ethmoid and the distal end of the occipital; neurocranium width (NCW), the distance between the outer edges of the pterosphenoid on both posterior sides; ethmoid length (EML), the distance from the tip of the ethmoid to the

groove between the ethmoid and the frontals; orbit length (OBL), the maximum distance of the eye level; pre-orbit length (POBL), distance from the front of the orbital to the tip of premaxilla; maximum premaxillary-ethmovomer width (MPEVW), the maximum width from anteriormost part of premaxillary-ethmovomer; maximum frontal width (MFW), the maximum width from anterior wings of frontals; neurocranium depth at basisphenoid (NCDB), the greatest depth from top of frontals to the parasphenoid or the base of vomer at basisphenoid region; and mid pre-orbital depth (mPOBD), depth at the middle part of orbital region (Fig 2). These measurements were done using digital calipers to the nearest 0.01 mm.

To determine the length ratios and their relation in terms of sizes, the neurocranium length was used to divide by neurocranium width, ethmoid length, orbit length, pre-orbit length, maximum premaxillary-ethmovomer width, maximum frontal width, neurocranium depth at basisphenoid, and mid pre-orbital depth (Table 1). The neurocranium lengths and morphological characters were evaluated. Some of the specimens displayed a ruptured braincase due to the extraction of the otolith, but these did not hinder the collection of data from the neurocranium. The morphological terminologies on diagnosis follow Böhlke *et al.* (1989).

Results

Morphometric and morphological diagnosis on the neurocranium of 34 muraenid species

1. Genus *Echidna*

1.1 *Echidna nebulosa* (Ahl, 1789) (Fig. 3 A–B)

Specimens examined and length measurements: Six samples. TOU-AE 061, 44.7 cm; TOU-AE 213, 73.4 cm; TOU-AE 5193, 54.0 cm; TOU-AE 5195, 56.5 cm; TOU-AE 5243, 56.5 cm; TOU-AE 5256, 56.0 cm; all in TL. NCL: 27.21–53.73 mm; NCW: 7.89–14.87 mm; EML: 11.5–23.34 mm; OBL: 4.0–8.45 mm; POBL: 6.34–12.84 mm; MPEVW: 4.51–9.82 mm; MFW: 4.26–8.12 mm; NCDB: 6.35–11.39 mm; and mPOBD: 3.36–7.03 mm.



FIGURE 3. Dorsal and left lateral view of *Echidna nebulosa* TOU-AE 0213, 73.4 cm TL. (A, B) and *E. polyzona* TOU-AE 4147, 52.9 cm TL. (C, D).

Diagnosis: PEV plate is short and oval in shape. Shallow groove situated at the posterior end of ethmoid. Presence of small pore at the joint between ethmoid and frontals. Ethmoid from tip of snout through the anterior of orbit has a small protrusion. Posterior end of the paired frontals has small pores. The parietals have a serrated margin with the paired frontals. The median crest of the supraoccipital extends anteriorly to the middle of parietal and ends with a small pore. Vomerine teeth are molariform.

1.2 *Echidna polyzona* (Richardson, 1845b) (Fig. 3 C–D)

Specimens examined and length measurements: Two samples. TOU-AE 3725, 42.8 cm and TOU-AE 4147, 52.9 cm; all in TL. NCL: 33.14–41.16 mm; NCW: 7.7–9.77 mm; EML: 15.39–18.03 mm; OBL: 5.28–6.08 mm; POBL: 7.77–9.21 mm; MPEVW: 4.95–6.32 mm; MFW: 5.37–6.72 mm; NCDB: 7.84–9.72 mm; and mPOBD: 4.26–4.98 mm.

Diagnosis: Groove in the posterior end of ethmoid is present. Protruding ridge between the paired frontals runs through supraoccipital. At least two sets of small pores were present at the anterior part of the frontals and one pair at the middle part. Margins between frontals and parietals were highly serrated. The paired sphenotics were reduced and descend downward. Pterosphenoïd has a small pore on its posterior part. Supraoccipital bears a median crest projecting upward and was higher than pterotic. Premaxillary and vomerine teeth are short and blunt. Neurocranium has a light purple coloration.

2. Genus *Enchelycore*

2.1 *Enchelycore lichenosa* (Jordan & Snyder, 1901) (Fig. 4 A–B)

Specimens examined and length measurements: One sample. TOU-AE 5128, 65.6 cm TL. NCL: 49.13 mm; NCW: 11.52 mm; EML: 26.18 mm; OBL: 7.69 mm; POBL: 15.58 mm; MPEVW: 8.96 mm; MFW: 11.8 mm; NCDB: 8.13 mm; and mPOBD: 4.16 mm.

Diagnosis: Ethmoid has a flat surface with a shallow groove on its posterior end. Protruding ridge between paired frontals runs through parietals. Basisphenoid has a small, sharp process. Parietals bear a small pore on midline. The sphenotic slightly overlies the anterolateral surface of the pterotic. It is situated on the midline and the extended process is facing backwards. Supraoccipital is short and stout and slightly higher than pterotic. Lateral view displayed an angled position of ethmoid from the tip of premaxilla. Premaxillary teeth are very slender and pointed. Vomerine teeth are uniformly short and sharp.

2.2 *Enchelycore pardalis* (Temminck & Schlegel, 1846) (Fig. 4 C–D)

Specimens examined and length measurements: Two samples. TOU-AE 5145, 68.5 cm; TOU-AE 7339, 74.5 cm; all in TL. NCL: 57.1–58.32 mm; NCW: 13.96–15.78 mm; EML: 30.05–30.06 mm; OBL: 9.56–11.14 mm; POBL: 18.97–20.55 mm; MPEVW: 7.87–9.64 mm; MFW: 10.17–10.47 mm; NCDB: 10.84–12.02 mm; and mPOBD: 4.6–5.1 mm.

Diagnosis: PEV plate is elongated. Shallow groove at posterior end of ethmoid is present. Slightly higher ridge can be seen between paired frontals. Basisphenoid has an outgrown small process toward PEV. Supraoccipital is short and stout. The dorsal part of epiotic and proximal end of supraoccipital is flat. Sphenotic has no extended process and situated midline. Premaxillary and vomerine teeth are long and sharp.

2.3 *Enchelycore schismatorhynchus* (Bleeker, 1853) (Fig. 4 E–F)

Specimens examined and length measurements: One sample. TOU-AE 3717, 30.3 cm TL. NCL: 56.62 mm; NCW: 17.25 mm; EML: 34.07 mm; OBL: 10.41 mm; POBL: 21.16 mm; MPEVW: 11.24 mm; MFW: 16.07 mm; NCDB: 12.03 mm; and mPOBD: 8.07 mm.

Diagnosis: PEV plate is long and cone-shaped. Paired frontals have slightly higher ridge in between. Parietals have some paired pores and half of the posterior end bears a ridge that runs through supraoccipital. Supraoccipital median crest is short and stout but higher than pterotic. Epiotic has a very short posterodorsal prolongation which is aligned with the proximal end of supraoccipital. Sphenotic has no distal expansion. Paired pterosphenoids have a sharp edge projecting downward. Premaxillary and vomerine teeth are long and sharp.

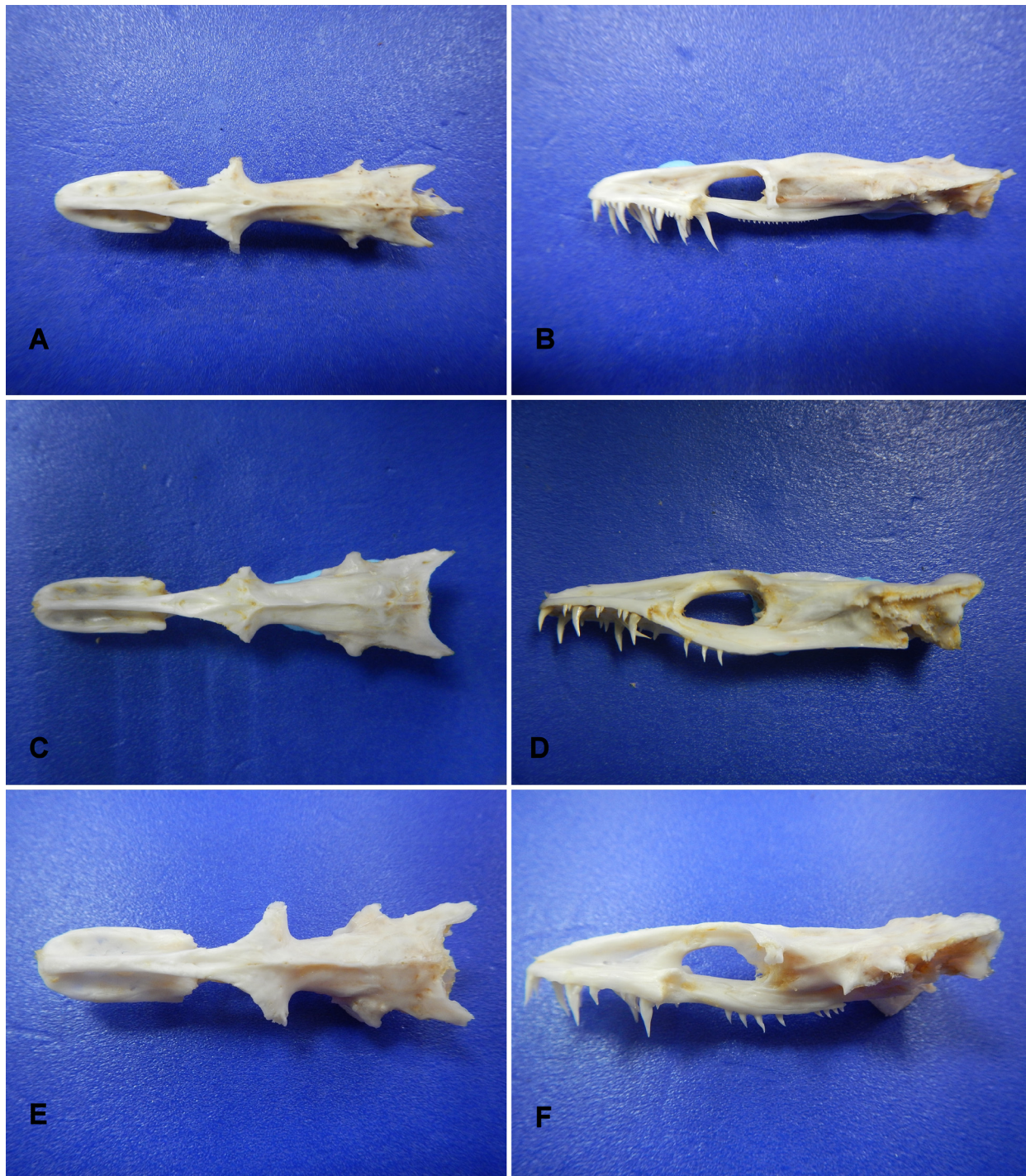


FIGURE 4. Dorsal and left lateral view of *Enchelycore lichenosa* TOU-AE 5128, 65.6 cm TL. (A, B), *E. pardalis* 5145, 68.5 cm TL. (C, D) and *E. schismatorhynchus* 3717, 30.3 cm TL. (E, F).

3. Genus *Gymnomuraena*

3.1 *Gymnomuraena zebra* (Shaw, 1797) (Fig. 5 A–B)

Specimens examined and length measurements: One sample. TOU-AE 4335, 84.4 cm TL. NCL: 62.54 mm; NCW: 13.77 mm; EML: 22.43 mm; OBL: 5.75 mm; POBL: 11.48 mm; MPEVW: 8.92 mm; MFW: 6.41 mm; NCDB: 11.32 mm; and mPOBD: 6.03 mm.

Diagnosis: PEV plate is short and round in shape. Protruding ridge between paired frontals runs through supraoccipital. Midline of paired parietals has small pore. Dorsal part of supraoccipital is longer than the pterotic. It bears a blade-shaped crest that extends dorsally. The pterosphenoid, sphenotic, and pterotic have downward projections, making each appear slender in the dorsal view and deeper on the lateral side. Oblong shape of vomer is visible from the dorsal view. Premaxillary and vomerine teeth are molariform. Neurocranium has a light purple coloration.

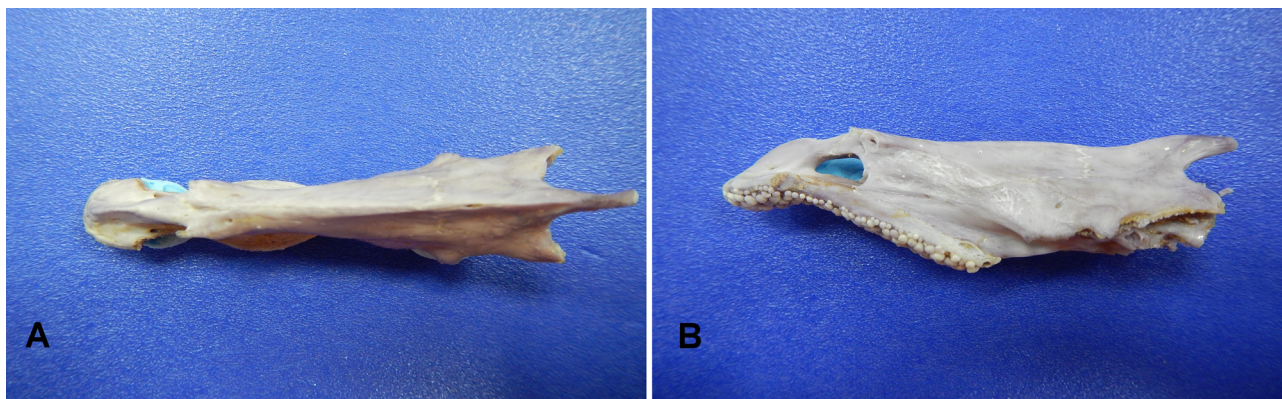


FIGURE 5. Dorsal and left lateral view of *Gymnomuraena zebra* TOU-AE 4335, 84.4 cm TL. (A, B).

4. Genus *Gymnothorax*

4.1 *Gymnothorax albimarginatus* (Temminck & Schlegel, 1846) (Fig. 6 A–B)

Specimens examined and length measurements: One sample. TOU-AE 5323, 106.0 cm TL. NCL: 53.91 mm; NCW: 17.39 mm; EML: 27.07 mm; OBL: 10.58 mm; POBL: 18.18 mm; MPEVW: 15.94 mm; MFW: 16.68 mm; NCDB: 12.9 mm; and mPOBD: 6.0 mm.

Diagnosis: PEV plate is oval in shape. Ethmoid surface is angled. A deeper groove which appears outlined by folded layer bones is present on the posterior end of the ethmoid. Basisphenoid has an outgrown small process toward PEV. Supraoccipital is short and stout but protruding posteriorly from the margin of parietal. Paired pore is present at the joint of pterosphenoid and sphenotic. Premaxillary and vomerine teeth are long and sharp.

4.2 *Gymnothorax berndti* Snyder, 1904 (Fig. 6 C–D)

Specimens examined and length measurements: Two samples. TOU-AE 4983, 73.0 cm; TOU-AE 4985, 67.4 cm; all in TL. NCL: 49.46–51.71 mm; NCW: 12.98–13.48 mm; EML: 26.06–26.49 mm; OBL: 8.71–9.12 mm; POBL: 15.63–15.67 mm; MPEVW: 7.96–9.02 mm; MFW: 9.34–10.31 mm; NCDB: 8.91–9.74 mm; and mPOBD: 5.93–7.66 mm.

Diagnosis: PEV plate is elongated. There is a small pore at the joint between the ethmoid and frontal bones. Ethmoid displayed overlapping groove at the posterior end. Basisphenoid has an outgrown small process toward PEV. Supraoccipital median crest is higher than pterotic. Sphenotic has small process extended midline. The edge of pterosphenoid is blunt. Premaxillary and vomerine teeth are long and sharp.

4.3 *Gymnothorax buroensis* (Bleeker, 1857) (Fig. 6 E–F)

Specimens examined and length measurements: Two samples. TOU-AE 2763, 26.3 cm; TOU-AE 7390, 25.0 cm; all in TL. NCL: 18.38–19.76 mm; NCW: 5.94–6.06 mm; EML: 9.68–9.94 mm; OBL: 2.89–3.72 mm; POBL: 4.98–5.03 mm; MPEVW: 3.95–4.22 mm; MFW: 4.68–5.18 mm; NCDB: 4.42–4.88 mm; and mPOBD: 2.75–2.85 mm.

Diagnosis: More cylindrical in shape from dorsal part of frontals posteriorly to parietals. PEV plate is short and cone-shaped. Its ethmoid connection is angled; frontal connection site has a ridge. Pore in the joint of ethmoid and frontals is present. Supraoccipital median crest is short and stout but higher than pterotic. Sphenotic has small process extended midline. Premaxilla and vomerine teeth are short and blunt. Neurocranium has a glossy and smooth surface.

4.4 *Gymnothorax chilospilus* Bleeker, 1864 (Fig. 6 G–H)

Specimens examined and length measurements: One sample. TOU-AE 5164, 55.5 cm TL. NCL: 24.28 mm; NCW: 6.53 mm; EML: 13.0 mm; OBL: 3.68 mm; POBL: 7.55 mm; MPEVW: 5.01 mm; MFW: 5.47 mm; NCDB: 4.78 mm; and mPOBD: 3.73 mm.

Diagnosis: PEV plate is short and cone-shaped. There is a pore in the joint between the ethmoid and the frontals. Paired parietals are oval in shape with a small pore at the joint. Posterior part of paired parietals is thinner than usual. A dark angled line can be seen on each side of the pterotic. Supraoccipital is short and stout. Premaxillary and vomerine teeth are long and sharp.

4.5 *Gymnothorax eurostus* (Abbott, 1860) (Fig. 6 I–J)

Specimens examined and length measurements: Four samples. TOU-AE 5315, 45.0 cm; TOU-AE 5316, 40.0 cm; TOU-AE 5317, 45.0 cm; TOU-AE 5329, 50.0 cm; all in TL. NCL: 29.75–36.25 mm; NCW: 9.18–12.33 mm; EML: 16.04–20.14 mm; OBL: 5.31–5.87 mm; POBL: 8.21–11.14 mm; MPEVW: 6.61–8.84 mm; MFW: 7.88–10.88 mm; NCDB: 6.57–7.96 mm; and mPOBD: 3.99–5.59 mm.

Diagnosis: A tiny slit horizontally is present on the groove at the posterior end of ethmoid. There is a pore in the joint between the ethmoid and the frontals. Paired parietal has a small pore at the joint. Supraoccipital is short and stout but higher than the pterotic. Paired pterotics posterodorsally have an ascending process. Sphenotic has small process extended midline. Premaxillary and vomerine teeth are long and sharp.

4.6 *Gymnothorax favagineus* Bloch & Schneider, 1801 (Fig. 7 A–B)

Specimens examined and length measurements: Two samples. TOU-AE 7473, 73.1 cm; TOU-AE 7374, 67.8 cm; all in TL. NCL: 47.52–49.62 mm; NCW: 13.56–14.04 mm; EML: 22.7–24.61 mm; OBL: 7.03–7.25 mm; POBL: 11.87–12.46 mm; MPEVW: 8.74–8.98 mm; MFW: 12.31–12.88 mm; NCDB: 9.55–9.68 mm; and mPOBD: 6.08–6.25 mm.

Diagnosis: Surface of ethmoid appears flat and has wider width. Ridge between the paired frontals runs through supraoccipital. Midline on the posterior end of paired parietals has small paired pores. Supraoccipital bears a median crest projecting upward and was higher than pterotic. Wider curve can be seen between the dorsal part of supraoccipital and pterotic. Paired pterosphenoid have a sharp edge. Sphenotic has small process extended midline. Premaxillary and vomerine teeth are long and sharp.

4.7 *Gymnothorax fimbriatus* (Bennett, 1832) (Fig. 7 C–D)

Specimens examined and length measurements: Three samples. TOU-AE 3705, 63.1 cm; TOU-AE 3713, 71.4 cm; TOU-AE 4243, 67.2 cm; all in TL. NCL: 51.28–54.75 mm; NCW: 13.97–15.65 mm; EML: 26.57–29.53 mm; OBL: 15.62–16.8 mm; POBL: 9.43–11.25 mm; MPEVW: 8.4–9.39 mm; MFW: 10.3–13.28 mm; NCDB: 9.7–11.24 mm; and mPOBD: 5.23–6.23 mm.

Diagnosis: PEV plate is oblong in shape. Anterodorsal of ethmoid is slightly wide. A small pore is visible on PEV right under the orbit. Shallow groove situated at the posterior end of ethmoid. High ridge at the joint of paired frontals extends until supraoccipital. Basisphenoid has an outgrown small process toward PEV. Lateral view displayed an angled position of ethmoid from the tip of pointed premaxilla. Premaxillary and vomerine teeth are long and sharp.



FIGURE 6. Dorsal and left lateral view of *Gymnothorax albimarginatus* TOU-AE 5323, 106.0 cm TL. (A, B); *G. berndti* TOU-AE 4983, 73.0 cm TL. (C, D); *G. buroensis* TOU-AE 2763, 26.3 cm TL. (E, F); *G. chilospilus* TOU-AE 5164, 55.5 cm TL. (G, H); *G. eurostus* TOU-AE 5315, 45.0 cm TL. (I, J).

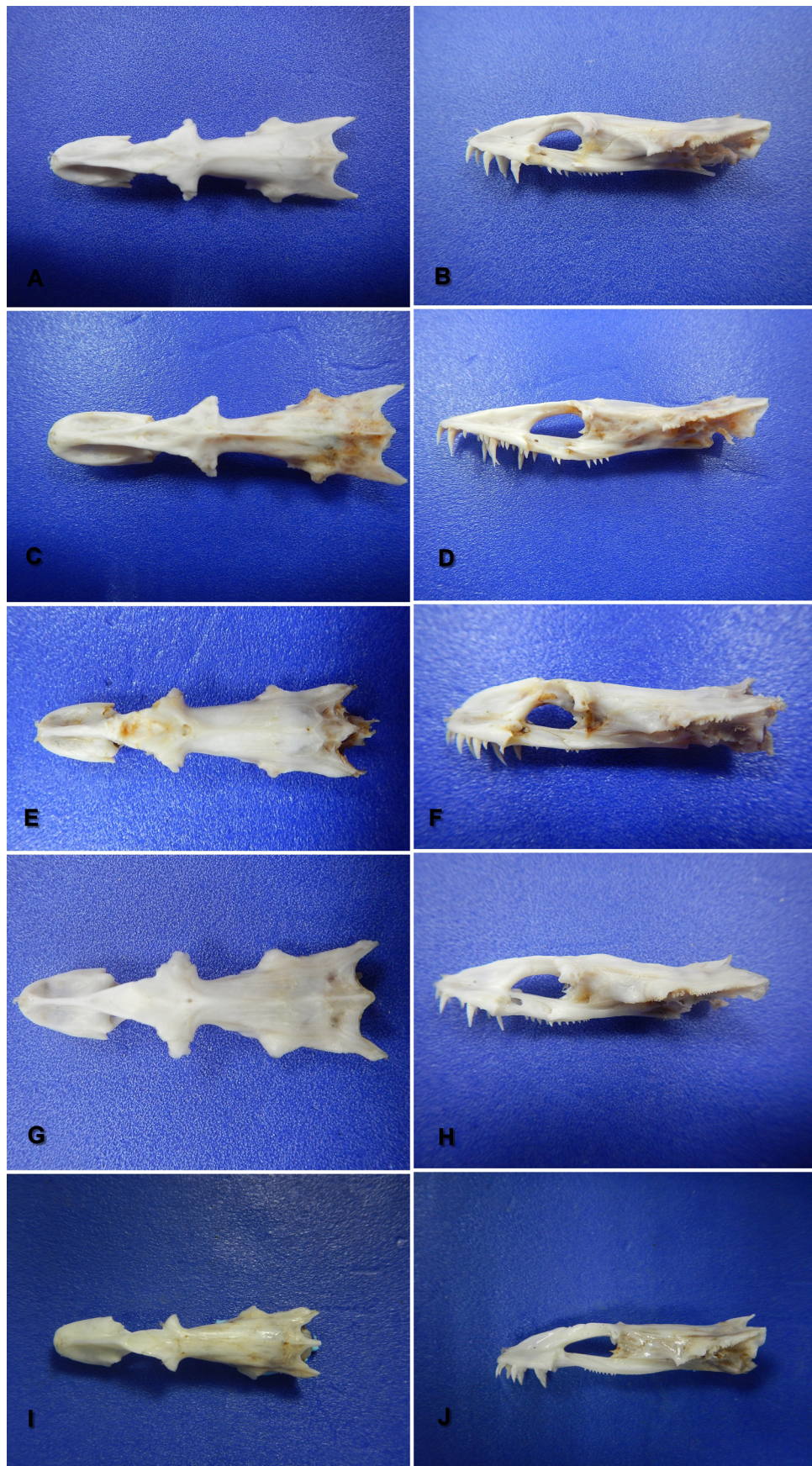


FIGURE 7. Dorsal and left lateral view of *Gymnothorax favagineus* TOU-AE 7474, 67.8 cm TL. (A, B); *G. fimbriatus* TOU-AE 3713, 71.4 cm TL. (C, D); *G. flavimarginatus* TOU-AE 7409, 51.1 cm TL. (E, F); *G. formosus* TOU-AE 7482, 75.1 cm TL. (G, H); *G. intesi* TOU-AE 5148, 65.0 cm TL. (I, J).

4.8 *Gymnothorax flavimarginatus* (Rüppell, 1830) (Fig. 7 E–F)

Specimens examined and length measurements: One sample. TOU-AE 7409, 51.1 cm TL. NCL: 34.83 mm; NCW: 9.73 mm; EML: 17.19 mm; OBL: 5.35 mm; POBL: 8.38 mm; MPEVW: 6.74 mm; MFW: 8.98 mm; NCDB: 7.73 mm; and mPOBD: 6.23 mm.

Diagnosis: PEV plate is short and oval in shape. Posterior end of ethmoid has a groove with rough surface. Lateral side displayed a small protrusion in between the premaxillary-ethmovomer and frontals. Paired pores are present at the joint of ethmoid and paired frontals. Margins between frontals and parietals were highly serrated. Supraoccipital median crest is short but higher than pterotic. Sphenotic has no distal expansion. The edge of paired pterosphenoids is blunt. Premaxillary and vomerine teeth are long and sharp.

4.9 *Gymnothorax formosus* Bleeker, 1864 (Fig. 7 G–H)

Specimens examined and length measurements: Two samples. TOU-AE 1860, 75.8 cm; TOU-AE 7482, 75.1 cm. all in TL. NCL: 34.14–40.74 mm; NCW: 11.11–14.1 mm; EML: 16.26–20.3 mm; OBL: 5.45–8.11 mm; POBL: 8.77–9.98 mm; MPEVW: 7.87–8.74 mm; MFW: 7.18–11.68 mm; NCDB: 7.68–9.03 mm; and mPOBD: 4.41–4.66 mm.

Diagnosis: PEV plate is short and oval in shape. Remarkable pore at the middle of paired frontals is present. Basisphenoid has an outgrown small process toward PEV. Frontals and parietals are separated with serrated margins. Supraoccipital median crest is short but higher than pterotic. Epiotic has a very short posterodorsal prolongation which is aligned with the proximal end of supraoccipital. Paired pterotics posterodorsally have an ascending process. Sphenotic has no distal expansion. The edge of paired pterosphenoids is blunt. Premaxillary and vomerine teeth are long and sharp.

4.10 *Gymnothorax intesi* (Fourmanoir & Rivaton, 1979) (Fig. 7 I–J)

Specimens examined and length measurements: Four samples. TOU-AE 5069, 43.3 cm; TOU-AE 5148, 65.0 cm; TOU-AE 5151, 40.2 cm; TOU-AE 5325, 47.0 cm; all in TL. NCL: 24.08–38.63 mm; NCW: 6.13–10.42 mm; EML: 11.73–16.05 mm; OBL: 4.04–8.0 mm; POBL: 6.12–10.16 mm; MPEVW: 4.04–7.45 mm; MFW: 4.19–8.2 mm; NCDB: 4.35–7.59 mm; and mPOBD: 2.21–4.34 mm.

Diagnosis: Ethmoid has a groove at the posterior end. Deep curve at the posterodorsal end of epiotic situated between parietal and supraoccipital. There is a pore on the margin between supraoccipital and parietal. Supraoccipital median crest is projecting upward. Sphenotic has no distal expansion. Pterosphenoid has a small sharp end on each side. Premaxillary and vomerine teeth are long and sharp.

4.11 *Gymnothorax kidako* (Temminck & Schlegel, 1846) (Fig. 8 A–B)

Specimens examined and length measurements: Two samples. TOU-AE 7575, 71.4 cm; TOU-AE 7576, 71.0 cm; all in TL. NCL: 47.04–47.63 mm; NCW: 13.11–13.97 mm; EML: 25.58–27.73 mm; OBL: 7.46–7.55 mm; POBL: 15.15–15.29 mm; MPEVW: 8.99–9.42 mm; MFW: 10.32–10.33 mm; NCDB: 8.73–9.41 mm; and mPOBD: 5.18–5.2 mm.

Diagnosis: Ethmoid has a flat surface with a shallow groove on its posterior end. Paired frontals are connected by a ridge and anterior part bears a paired pore. Basisphenoid has an outgrown small process toward PEV. Shallow curve on the posterodorsal end of epiotic situated between parietal and supraoccipital. Supraoccipital median crest is short but higher than pterotic. Sphenotic has no distal expansion. Pterosphenoid has a blunt end on each side. Premaxillary and vomerine teeth are long and sharp.

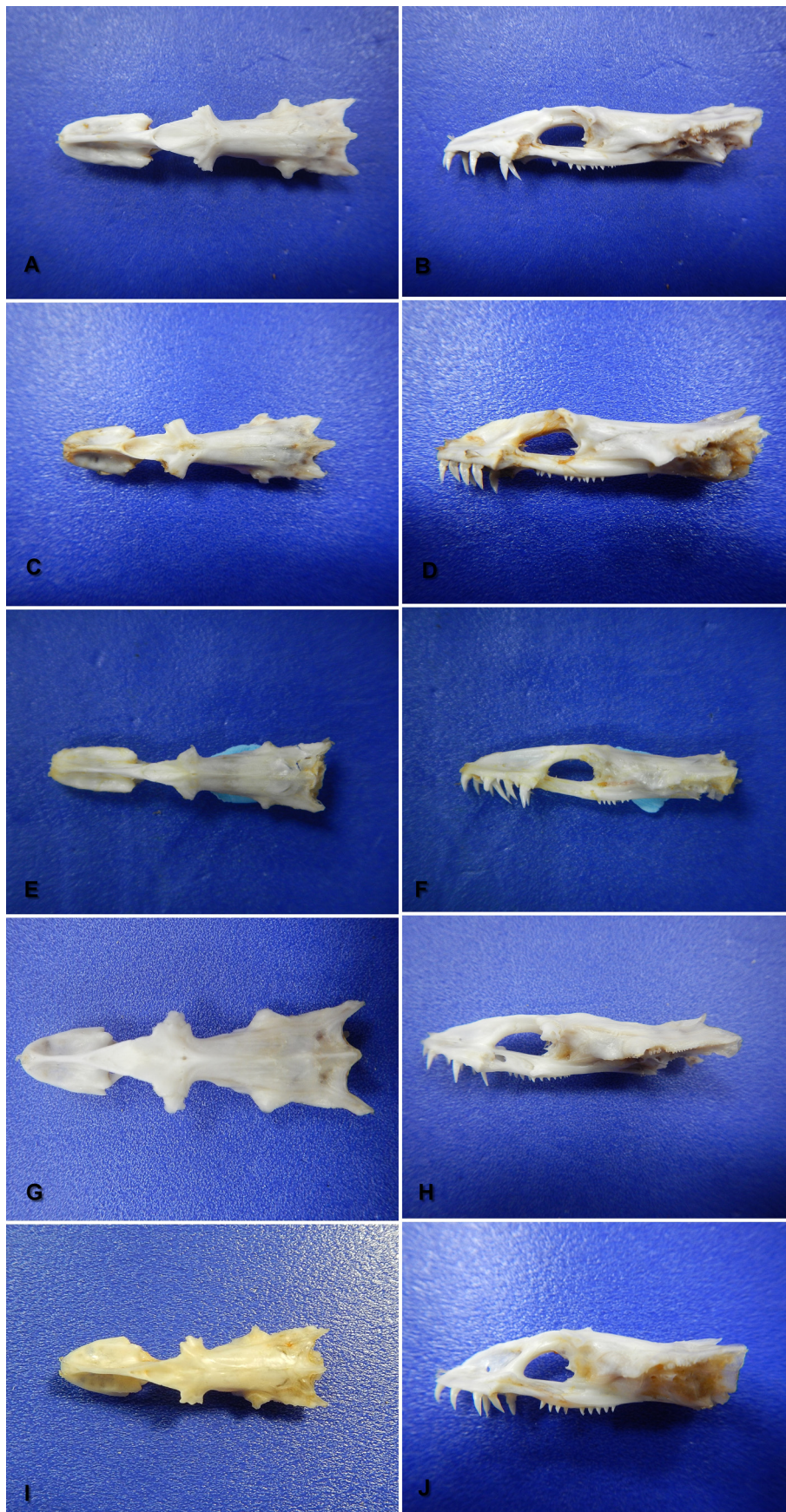


FIGURE 8. Dorsal and left lateral view of *Gymnothorax kidako* TOU-AE 7576, 71.1 cm TL. (A, B); *G. leucostigma* TOU-AE 7333, 70.0 cm TL. (C, D); *G. margaritophorus* TOU-AE 3243, 38.3 cm TL. (E, F); *G. meleagris* TOU-AE 7338, 75.0 cm TL. (G, H), *G. minor* TOU-AE 7319, 51.4 cm TL. (I, J).

4.12 *Gymnothorax leucostigma* Jordan & Richardson, 1909 (Fig. 8 C–D)

Specimens examined and length measurements: Two samples. TOU-AE 7332, 52.9 cm; TOU-AE 7333, 70.0 cm; all in TL. NCL: 35.58–45.68 mm; NCW: 8.93–11.5 mm; EML: 20.05–26.89 mm; OBL: 7.12–7.87 mm; POBL: 9.39–12.22 mm; MPEVW: 7.17–8.8 mm; MFW: 7.78–8.29 mm; NCDB: 7.02–8.67 mm; and mPOBD: 4.49–5.6 mm.

Diagnosis: PEV plate is cone-shaped. Pore is present at the joint of ethmoid and paired frontals. Anterodorsal part of frontals have at least two paired pores. Basisphenoid has an outgrown small process toward PEV. Margin between paired frontals and parietals are connected by serrated line. Supraoccipital median crest is short and projects upward. Paired pterotics posterodorsally have an ascending process. Sphenotic has extended process facing backward. Paired pterosphenoids have a sharp edge projecting downward and a paired pore near sphenotic. Premaxillary and vomerine teeth are long and sharp.

4.13 *Gymnothorax margaritophorus* Bleeker, 1864 (Fig. 8 E–F)

Specimens examined and length measurements: One sample. TOU-AE 3243, 38.3 cm TL. NCL: 27.63 mm; NCW: 7.23 mm; EML: 15.21 mm; OBL: 4.54 mm; POBL: 9.31 mm; MPEVW: 4.63 mm; MFW: 5.25 mm; NCDB: 5.78 mm; and mPOBD: 3.5 mm.

Diagnosis: PEV plate is oblong in shape. Ethmoid has a thin surface with a groove at the posterior end. A dark angled line can be seen on each side of the pterotic. Supraoccipital is short and stout but slightly higher than pterotic. Sphenotic has no distal expansion. Paired pterosphenoid has blunt end. Premaxillary and vomerine teeth are long and sharp.

4.14 *Gymnothorax meleagris* (Shaw, 1795) (Fig. 8 G–H)

Specimens examined and length measurements: One sample. TOU-AE 7338, 75.0 cm TL. NCL: 53.77 mm; NCW: 15.37 mm; EML: 27.74 mm; OBL: 9.31 mm; POBL: 14.05 mm; MPEVW: 11.4 mm; MFW: 14.31 mm; NCDB: 11.37 mm; and mPOBD: 6.44 mm.

Diagnosis: PEV plate is cone-shaped. Ethmoid has a deep groove with a slit at the posterior end. There is a pore at the joint of ethmoid and the paired frontals. The parietals have a serrated margin from the paired frontals, small pore is present at the posterior end. Supraoccipital is short and stout and almost aligned with the proximal end of pterotic. The sphenotic has an extended process facing downwards. Pterosphenoid has sharp edge and posterior part has pore. Premaxillary and vomerine teeth are long and sharp.

4.15 *Gymnothorax minor* (Temmick & Schlegel, 1846) (Fig. 8 I–J)

Specimens examined and length measurements: Two samples. TOU-AE 7319, 51.4 cm; TOU-AE 5032, 48.2 cm, all in TL. NCL: 26.5–28.57 mm; NCW: 8.23–8.88 mm; EML: 11.96–15.5 mm; OBL: 4.44–4.54 mm; POBL: 7.61–8.8 mm; MPEVW: 5.06–6.53 mm; MFW: 5.51–6.73 mm; NCDB: 6.95–7.97 mm; and mPOBD: 4.19–4.31 mm.

Diagnosis: PEV plate is oval in shape. Ethmoid has a thin surface with a groove on its posterior end. Lateral part of ethmoid, surface of PEV plate and posterodorsal of parietal nearly transparent. There is a pore at the joint between ethmoid and paired frontals, paired pores displayed near the ridge. Supraoccipital median crest is short but higher than the parietals. Deep curve at the edge of epiotic at its posterodorsal end. Sphenotic has extended process. Pterosphenoid has blunt end. Premaxillary and vomerine teeth are long and sharp. Neurocranium displays glossy, light yellow coloration.

4.16 *Gymnothorax monochrous* (Bleeker, 1856) (Fig. 9 A–B)

Specimens examined and length measurements: Four samples. TOU-AE 5079, 50.5 cm; TOU-AE 5157, 58.5 cm;

TOU-AE 5231, 71.5 cm; TOU-AE 5324, 53.5 cm; all in TL. NCL: 28.13–43.34 mm; NCW: 7.49–12.68 mm; EML: 9.53–22.52 mm; OBL: 4.79–8.08 mm; POBL: 9.31–13.46 mm; MPEVW: 5.19–8.16 mm; MFW: 6.07–12.36 mm; NCDB: 5.12–8.96 mm; and mPOBD: 3.68–4.75 mm.

Diagnosis: PEV plate is oblong in shape. Shallow groove at the posterior end of ethmoid. A pore is present at the joint of ethmoid and paired frontals. Orbit resembles half of an oblong shape, horizontally. Posterior part of parietals has pore at the midline. Supraoccipital median crest is thin, projecting upward and higher than the pterotic. Posterior part of paired parietals is thin. A dark angled line can be seen on each side of the pterotic. Sphenotic has small process that extends midline. The edge of paired pterosphenoids is sharp. Premaxillary and vomerine teeth are long and sharp.

4.17 *Gymnothorax mucifer* Snyder, 1904 (Fig. 9 C–D)

Specimens examined and length measurements: Four samples. TOU-AE 5175, 44.0 cm; TOU-AE 5176, 54.0 cm; TOU-AE 5348, 65.9 cm; TOU-AE 7477, 54.4 cm; all in TL. NCL: 32.4–46.74 mm; NCW: 8.16–13.35 mm; EML: 17.0–25.57 mm; OBL: 5.55–8.46 mm; POBL: 10.55–14.63 mm; MPEVW: 5.36–9.04 mm; MFW: 6.02–8.34 mm; NCDB: 5.8–9.26 mm; and mPOBD: 3.85–5.81 mm.

Diagnosis: PEV plate is elongated. Ethmoid has a thin surface and groove is present at the posterior end. Joint of paired frontal has a ridge and bears a paired pore at the anterodorsal part. Basisphenoid has a small sharp process. Parietals have some paired small pores. Supraoccipital is short and stout, and its median crest ascends higher than pterotic. Sphenotic has extended process facing downwards. Pterosphenoid has blunt end. Premaxillary and vomerine teeth are long and sharp.

4.18 *Gymnothorax neglectus* Tanaka, 1911 (Fig. 9 E–F)

Specimens examined and length measurements: Two samples. TOU-AE 7334, 47.9 cm; TOU-AE 7335, 49.5 cm, all in TL. NCL: 33.65–34.8 mm; NCW: 8.67–8.71 mm; EML: 17.87–18.71 mm; OBL: 5.25–5.95 mm; POBL: 10.87–11.34 mm; MPEVW: 5.38–6.04 mm; MFW: 6.46–6.88 mm; NCDB: 6.73–6.87 mm; and mPOBD: 3.0–3.98 mm.

Diagnosis: PEV plate is elongated. Ethmoid has a thin surface with a shallow groove at the posterior end. Paired frontals have a ridge in between. Basisphenoid has an outgrown process toward PEV. A dark angled line can be seen on each side of parietals. Supraoccipital median crest is short and stout but higher than pterotic. Sphenotic has no distal expansion. Pterosphenoid has blunt end. Premaxillary and vomerine teeth are long and sharp.

4.19 *Gymnothorax nudivomer* (Günther, 1867) (Fig. 9 G–H)

Specimens examined and length measurements: One sample. TOU-AE 7472, 65.2 cm TL. NCL: 38.56 mm; NCW: 10.15 mm; EML: 18.8 mm; OBL: 7.06 mm; POBL: 9.46 mm; MPEVW: 8.39 mm; MFW: 10.53 mm; NCDB: 8.67 mm; and mPOBD: 5.65 mm.

Diagnosis: PEV plate is oval in shape. There is a pore at the joint between the ethmoid and the frontals. Anterodorsal part of frontals has lateral process slightly extending downward, covering the upper part of orbit. Basisphenoid has an outgrown process toward PEV. Posterior part of paired parietals has small pore at the joint. Supraoccipital ascends posteriorly and higher than pterotic. Curve at the posterodorsal end of epiotic is deep. Sphenotic has no distal expansion. Pterosphenoid has sharp edge. Premaxillary teeth are long and sharp, vomerine teeth are absent.

4.20 *Gymnothorax pictus* (Ahl, 1789) (Fig. 9 I–J)

Specimens examined and length measurements: Two samples. TOU-AE 5282, 57.8 cm; TOU-AE 7366, 39.8 cm, all in TL. NCL: 23.52–36.3 mm; NCW: 6.28–9.81 mm; EML: 12.0–17.96 mm; OBL: 4.71–6.71 mm; POBL: 6.78–10.01 mm; MPEVW: 4.61–6.97 mm; MFW: 6.4–7.13 mm; NCDB: 5.73–7.36 mm; and mPOBD: 3.08–5.77 mm.

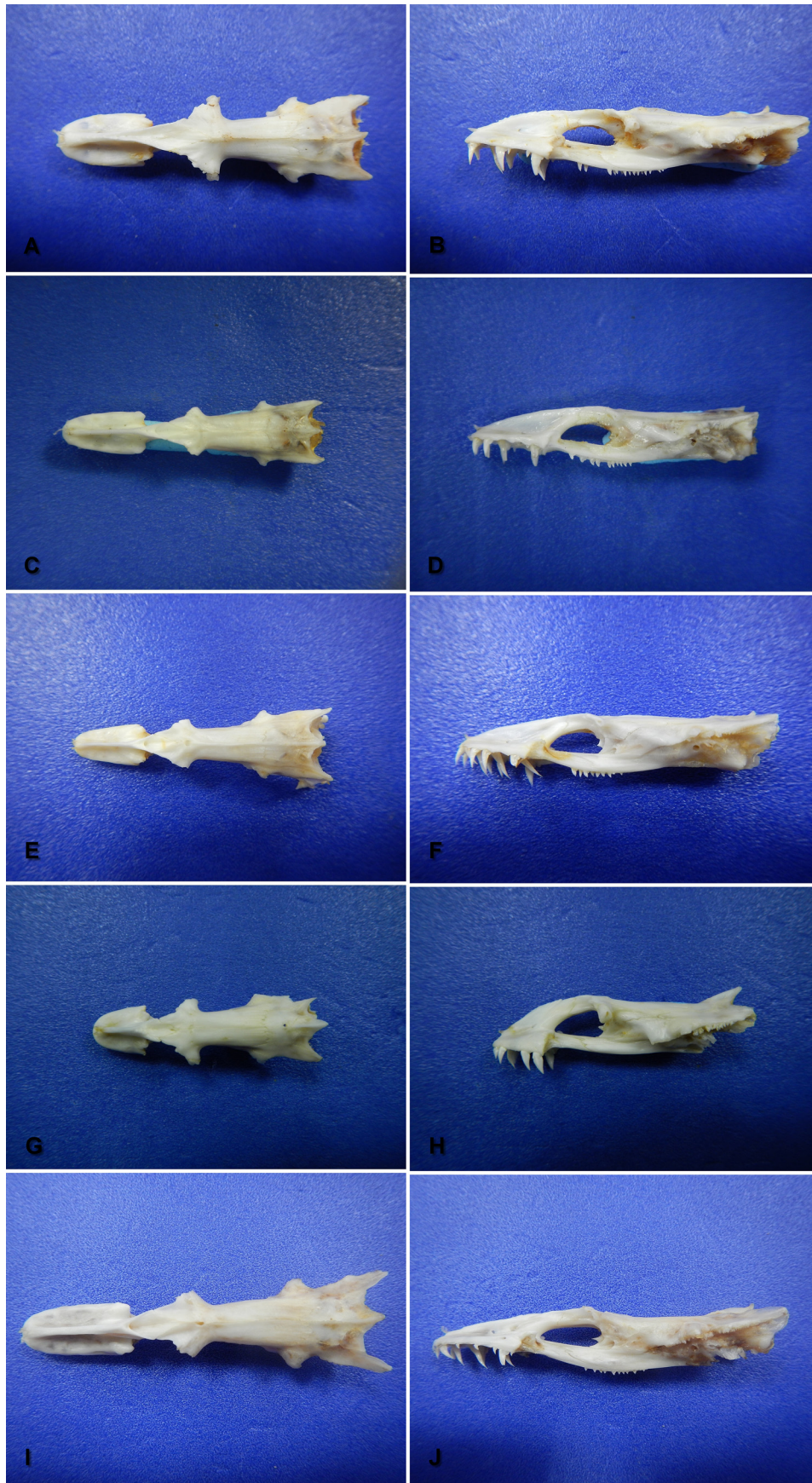


FIGURE 9. Dorsal and left lateral view of *Gymnothorax monochrous* TOU-AE 5231, 71.5 cm TL (A, B); *G. mucifer* TOU-AE 5175, 54.0 cm TL. (C, D); *G. neglectus* TOU-AE 7334, 47.9 cm TL. (E, F); *G. nudivomer* TOU-AE 7472, 65.2 cm TL. (G, H); *G. pictus* 5282, 57.8 cm TL. (I, J).

Diagnosis: PEV plate is triangular in shape. Ethmoid has a wide surface and shallow groove is present at the posterior end. Paired parietals have small pore at the joint, posterior end bears a ridge that runs through supraoccipital. Supraoccipital median crest is short but higher than pterotic. Epiotic has no posterodorsal prolongation and is slightly curved. Sphenotic has extended process facing backward. Pterosphenoid has a blunt end. Premaxillary and vomerine teeth are short but sharp.

4.21 *Gymnothorax pseudothyrsoides* (Bleeker, 1853) (Fig. 10 A–B)

Specimens examined and length measurements: Two samples. TOU-AE 6510, 53.9 cm; TOU-AE 7478, 63.5 cm; all in TL. NCL: 40.74–42.35 mm; NCW: 11.63–12.77 mm; EML: 20.68–21.46 mm; OBL: 6.95–7.39 mm; POBL: 12.07–12.35 mm; MPEVW: 8.49–9.98 mm; MFW: 11.61–12.73 mm; NCDB: 8.71–9.41 mm; and mPOBD: 5.37–5.32 mm.

Diagnosis: PEV plate is oval in shape. Ethmoid has shallow groove with a rough surface at the posterior end. There is a pore at the joint of ethmoid and frontals. Basisphenoid has an outgrown small process toward PEV. Supraoccipital median crest is short but protruding and higher than the pterotic. Epiotic has short posterodorsal prolongation and slightly curved. Sphenotic has extended process facing backward. Pterosphenoid has a sharp edge and pore is present at the posterior part. Premaxillary and vomerine teeth are long and sharp.

4.22 *Gymnothorax reevesii* (Richardson, 1845a) (Fig. 10 C–D)

Specimens examined and length measurements: Two samples. TOU-AE 7411, 65.3 cm; TOU-AE 7460, 74.7 cm, all in TL. NCL: 45.63–53.65 mm; NCW: 13.58–14.39 mm; EML: 22.36–26.72 mm; OBL: 8.43–8.83 mm; POBL: 13.37–14.89 mm; MPEVW: 11.91–13.03 mm; MFW: 14.94–14.97 mm; NCDB: 10.96–12.91 mm; and mPOBD: 5.49–6.61 mm.

Diagnosis: PEV plate is round in shape, surface is rough accompanied by several dark pitted circles. Ethmoid has a groove with an outgrown process. There is a pore in between ethmoid and paired frontal connection. Frontals display expanded lateral process which bear at least two pairs of pores. Basisphenoid has two outgrown process toward PEV. Parietals have one pair of pores at its posterior part and remarkable pore at the suture with supraoccipital. Supraoccipital median crest is short but higher than the pterotic. Edge of epiotic almost flat at its posterodorsal end, prolongation is minimal. Sphenotic has extended process facing downwards. Pterosphenoid has a sharp edge and pore is present at the posterior part. Premaxillary and vomerine teeth are long and sharp.

4.23 *Gymnothorax thyrsoides* (Richardson, 1845b) (Fig. 10 E–F)

Specimens examined and length measurements: Three samples. TOU-AE 5028, 46.1 cm; TOU-AE 5029, 47.2 cm; TOU-AE 7471, 54.5 cm, all in TL. NCL: 22.7–27.02 mm; NCW: 6.41–7.69 mm; EML: 10.42–13.18 mm; OBL: 3.33–4.16 mm; POBL: 5.91–6.78 mm; MPEVW: 4.3–5.71 mm; MFW: 4.4–5.13 mm; NCDB: 5.17–6.25 mm; and mPOBD: 3.46–3.63 mm.

Diagnosis: PEV plate is oval in shape. No ridge between paired frontals, instead a shallow marginal line can be seen. Remarkable expanded process from anterodorsal of frontals bears toward PEV. Supraoccipital median crest is higher than pterotic. Deep curve can be seen at the posterodorsal end of epiotic. Sphenotic has extended process facing downwards. Pterosphenoid has blunt end. Premaxillary and vomerine teeth are short, blunt, and stout. Neurocranium has light purple coloration and smooth surface.

4.24 *Gymnothorax undulatus* (Lacepède, 1803) (Fig. 10 G–H)

Specimens examined and length measurements: Two samples. TOU-AE 7461, 66.7 cm; TOU-AE 7462, 62.7 cm, all in TL. NCL: 49.35–51.29 mm; NCW: 12.6–13.2 mm; EML: 23.82–25.47 mm; OBL: 8.09–8.89 mm; POBL: 13.86–25.55 mm; MPEVW: 8.26–8.48 mm; MFW: 8.97–11.7 mm; NCDB: 9.35–9.72 mm; and mPOBD: 4.4–5.21 mm.

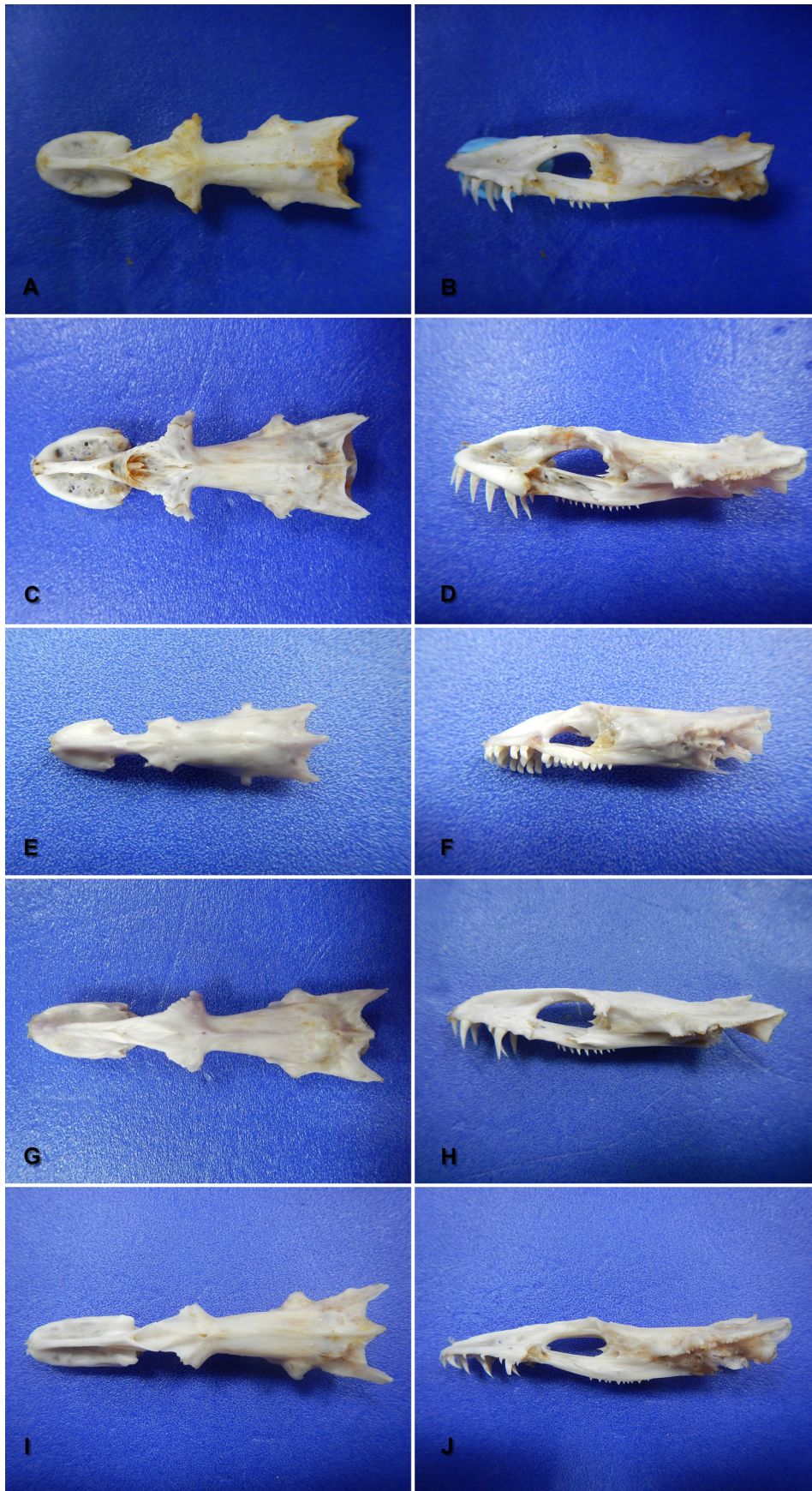


FIGURE 10. Dorsal and left lateral view of *Gymnothorax pseudothyrsoides* TOU-AE 6510, 53.9 cm TL. (A, B); *G. reevesii* 7411, 65.3 cm TL. (C, D); *G. thyrsoides* TOU-AE 7471, 54.5 cm TL. (E, F); *G. undulatus* TOU-AE 7461, 62.7 cm TL. (G, H), and *G. ypsilon* TOU-AE 7483, 101.8 cm TL. (I, J).

Diagnosis: PEV plate is elongated. Shallow groove with several lines is present at the posterior end of the ethmoid. Paired frontals are connected by a ridge. Pores are present on each side of the frontals and at the posterior end of the ridge. Basisphenoid has an outgrown process toward PEV. Supraoccipital has a pore on its anterior base, its median crest ascends higher than pterotic. Deep curve on the epiotic posterior end. Sphenotic has no distal expansion. Pterosphenoid has blunt end. Premaxillary and vomerine teeth are long and sharp.

4.25 *Gymnothorax ypsilon* Hatooka & Randall, 1992 (Fig. 10 I–J)

Specimens examined and length measurements: Two samples. TOU-AE 7483, 101.8 cm; TOU-AE 7484, 68.6 cm, all in TL. NCL: 45.52–59.69 mm; NCW: 11.56–15.96 mm; EML: 25.53–31.9 mm; OBL: 8.04–10.46 mm; POBL: 15.41–20.17 mm; MPEVW: 7.28–8.95 mm; MFW: 8.26–10.78 mm; NCDB: 7.7–10.82 mm; and mPOBD: 5.15–5.59 mm.

Diagnosis: PEV plate is elongated. Ethmoid has a thin surface with a groove on its posterior end. There is a pore at the joint of ethmoid and frontals. Basisphenoid has an outgrown process toward PEV. Supraoccipital median crest is short but higher than pterotic. Posterodorsal end of epiotic is almost flat. Sphenotic has no distal expansion. Pterosphenoid has blunt end. Premaxillary and vomerine teeth are long and sharp. Neurocranium is dorsally elongated and laterally compressed.

5. Genus *Scuticaria*

5.1 *Scuticaria tigrina* (Lesson, 1828) (Fig. 11 A–B)

Specimens examined and length measurements: One sample. TOU-AE 3245, 79.4 cm TL. NCL: 29.21 mm; NCW: 8.62 mm; EML: 13.48 mm; OBL: 4.14 mm; POBL: 7.78 mm; MPEVW: 6.57 mm; MFW: 5.92 mm; NCDB: 5.23 mm; and mPOBD: 1.98 mm.

Diagnosis: PEV plate is short and oval in shape. Lateral view displayed an angled position from the tip of premaxilla. Visible suture at the joint of paired frontals. Supraoccipital median crest is short and stout but higher than pterotic. Posterodorsal end of epiotic is almost flat line. Sphenotic has no distal expansion. Pterosphenoid has blunt end. Premaxillary and vomerine teeth are short but sharp.

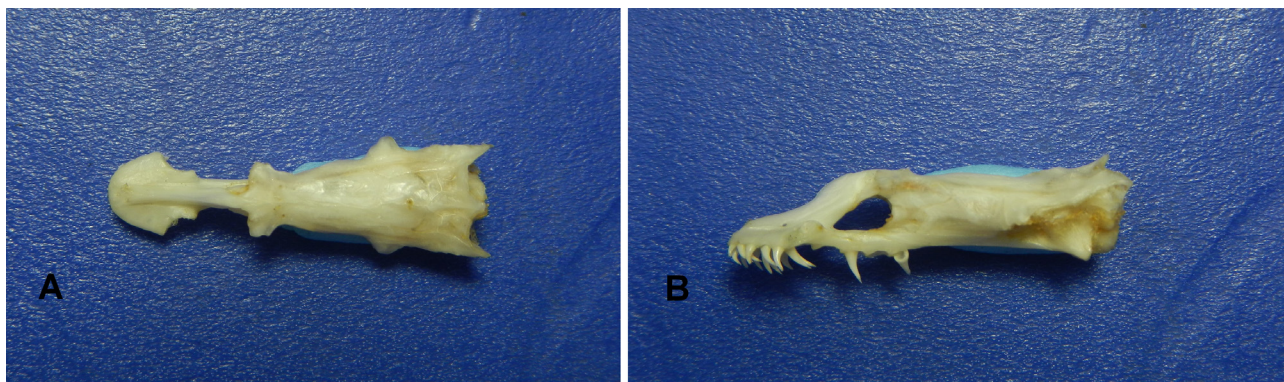


FIGURE 11. Dorsal and left lateral view of *Scuticaria tigrina* TOU-AE 3245, 79.4 cm TL. (A, B).

6. Genus *Strophidon*

6.1 *Strophidon sathete* (Hamilton, 1822) (Fig. 12 A–B)

Specimens examined and length measurements: One sample. TOU-AE 7435, 86.9 cm TL. NCL: 33.96 mm; NCW: 10.75 mm; EML: 16.54 mm; OBL: 5.48 mm; POBL: 8.46 mm; MPEVW: 7.44 mm; MFW: 8.03 mm; NCDB: 6.6 mm; and mPOBD: 5.12 mm.

Diagnosis: PEV plate is oval in shape with a pointed tip. Ethmoid has a thin surface and small protrusion anterior to PEV. Anterodorsal part of frontals has lateral process slightly extending downward, covering the upper part of orbit. Visible suture with remarkable pore at the joint of paired frontals. Posterodorsal end of epiotic is slightly curved. Supraoccipital median crest is short but higher than pterotic. Sphenotic has no distal expansion. Pterosphenoïd has blunt end. Premaxillary and vomerine teeth are short but sharp.

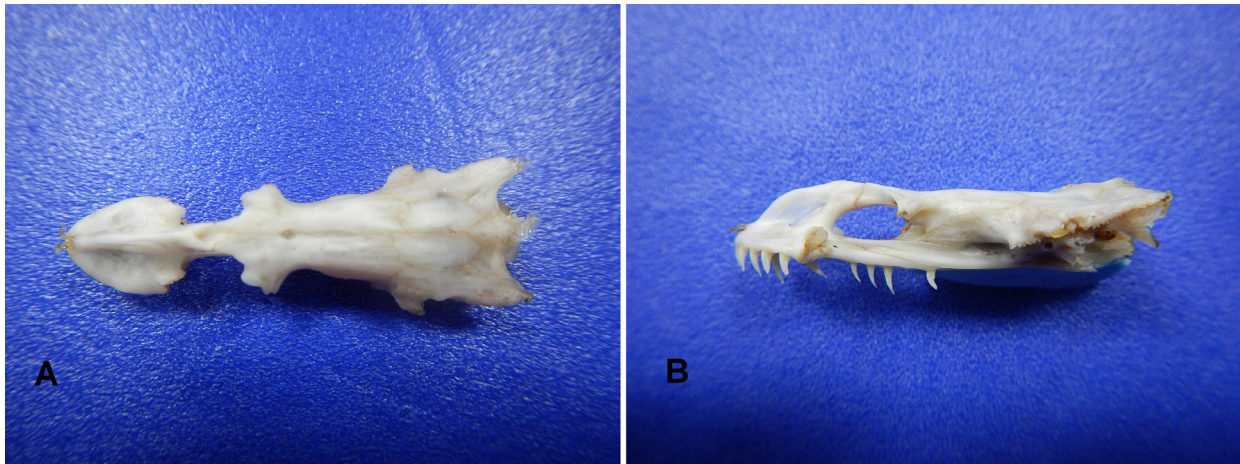


FIGURE 12. Dorsal and left lateral view of *Strophidon sathete* TOU-AE 7435, 86.9 cm TL. (A, B).

7. Genus *Uropterygius*

7.1 *Uropterygius macrocephalus* (Bleeker, 1864) (Fig. 13 A–B)

Specimens examined and length measurements: Three samples. TOU-AE 3214, 32.5 cm; TOU-AE 3219, 30.6 cm; TOU-AE 7391, 36.0 cm; all in TL. NCL: 17.94–23.03 mm; NCW: 5.27–6.43 mm; EML: 9.28–12.55 mm; OBL: 2.77–3.39 mm; POBL: 6.24–7.26 mm; MPEVW: 2.92–3.93 mm; MFW: 3.55–4.58 mm; NCDB: 4.11–5.33 mm; and mPOBD: 0.72–1.74 mm.

Diagnosis: PEV plate is elongated. Ethmoid has a thin surface which discontinued toward anterior part of PEV. Orbit is small. Visible suture at the joint of paired frontals. Posterodorsal line of epiotic is slightly curved with noticeable upward prolongation of supraoccipital, epiotics, and parietals. Supraoccipital median crest is higher than pterotic. Sphenotic has no distal expansion. Pterosphenoïd has blunt end. Premaxillary and vomerine teeth are short but sharp. Neurocranium has a ventral flattened basal plate from premaxilla toward parasphenoid.

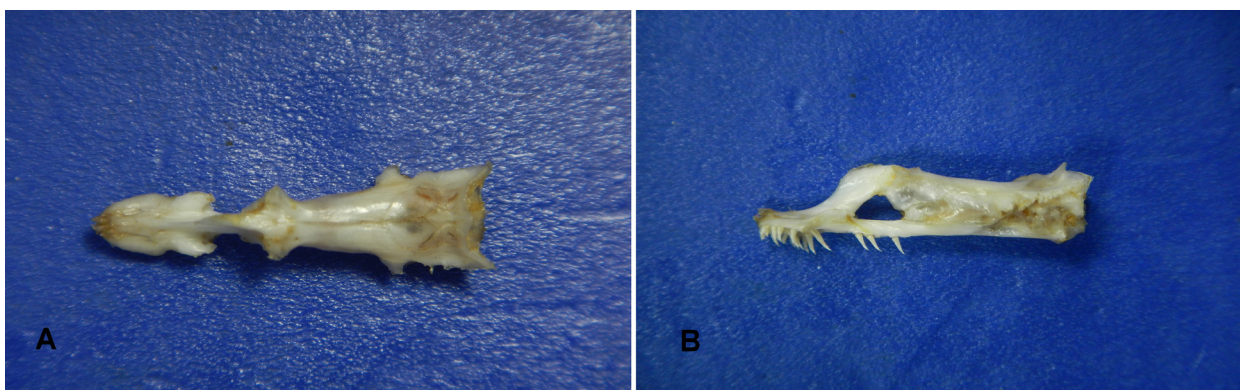


FIGURE 13. Dorsal and left lateral view of *Uropterygius macrocephalus* TOU-AE 7391, 36.0 cm TL. (A, B).

Osteology

The materials examined include 72 samples of muraenid species from six genera. Table 1 shows the list of moray

eel species with the average ratio of the measurements taken from NCL, NCW, EML, OBL, POBL, MPEVW, MFW, NCDB and mPOBD of each neurocranium. Average ratio of NCL to NCW shows maximum value for *Gymnomuraena zebra* (4.54) and minimum value for *Gymnothorax formosus* (2.98); ratio of NCL to EML shows maximum value for *Gymnomuraena zebra* (2.79) and minimum value for *Enchelycore schismatorhynchus* (1.66); ratio of NCL to OBL shows maximum value for *Gymnomuraena zebra* (10.88) and minimum value for *Gymnothorax albimarginatus* (5.1); ratio for NCL to POBL shows maximum value for *Gymnomuraena zebra* (5.45) and minimum value for *Enchelycore schismatorhynchus* (2.68); ratio of NCL to MPEVW shows maximum value for *Gymnomuraena zebra* (7.01) and minimum value for *Gymnothorax albimarginatus* (3.38); ratio of NCL to MFW shows maximum value for *Gymnomuraena zebra* (9.76) and minimum value for *Gymnothorax albimarginatus* (3.23); ratio of NCL to NCDB shows maximum value for *Enchelycore lichenosa* (6.04) and minimum value for *Gymnothorax minor* (3.7); and ratio of NCL and mPOBD shows maximum value for *Uropterygius macrocephalus* (19.82) and minimum value for *Gymnothorax flavimarginatus* (5.59).

Species of Uropterygiinae have the lowest measurements on mid pre-orbital depth and orbit length which resulted in the highest values on the relative ratio of the NCL to mPOBD and NCL to OBL ranging from 14.75–19.82 and 7.06–7.12, respectively. The unique characters were recorded on having a small orbit and the lowest value on the depth of mid pre-orbit due to the termination of the ethmoidal crest toward premaxilla (Fig. 16).

In Muraeninae, the species *Gymnothorax mucifer* was misidentified and synonymized as *G. kidako* also have differences based on relative ratio measurements, *Gymnothorax mucifer* is higher than *G. kidako* on the ratio of NCL/NCW (3.72>3.50); NCL/EML (1.86>1.78); NCL/POBL (3.17>3.11); NCL/MPEVW (5.63>5.14); and NCL/MFW (5.24>4.58), whereas *G. kidako* is higher in NCL/OBL (6.31>5.85); NCL/NCDB (5.22>5.17); and NCL/mPOBD (9.12>8.45). In morphological characters, *G. kidako* can be distinguished by having a wider and longer ethmoid surface than *G. mucifer*. Moreover, *Gymnomuraena zebra* and *Echidna* species share several characters that can distinguish them from other Muraeninae; for example, the relative ratio of the NCL to EML is 2.22–2.79, and the ethmoid is short, with its length being twice neurocranium length; and similarities on having molariform teeth (Fig. 25). However, the light purple coloration of the neurocranium is unobservable in *Echidna nebulosa*.

The neurocranium of moray eels is almost well ossified and truncated posteriorly, except where the exoccipital flanges break the contour of the neurocranium profile. The premaxilla, ethmoid, and vomer are fused, hence this combination is called premaxillary-ethmovomer (PEV). The PEV plate is laterally expanded, forming a downward-curving process. This character was observed for all of the specimens. Characters of individual species or groups of conspecifics (≤ 1) were thoroughly observed to obtain accurate coding. The round to oval shape of the PEV was observed from the dorsal view of *Echidna nebulosa*, *E. polyzona*, *Enchelycore lichenosa*, *Gymnomuraena zebra*, *Gymnothorax albimarginatus*, *G. buroensis*, *G. chilospilus*, *G. eurostus*, *G. favagineus*, *G. flavimarginatus*, *G. formosus*, *G. intesi*, *G. kidako*, *G. leucostigma*, *G. meleagris*, *G. monochrous*, *G. nudivomer*, *G. pictus*, *G. pseudothyrsoides*, *G. reevesii*, *G. thyrsoides*, *Scuticaria tigrina*, *Strophidon sathete*, and *Uropterygius macrocephalus*. The species *Enchelycore lichenosa*, *E. pardalis*, *E. schismatorhynchus*, *Gymnothorax berndti*, *G. fimbriatus*, *G. margaritophorus*, *G. mucifer*, *G. neglectus*, *G. undulatus*, and *G. ypsilon* were observed to have a cone-shaped premaxillary-ethmovomer (Fig. 18).

The angle of the premaxilla-ethmovomer from the tip of the premaxilla toward the frontals was assessed. The species *Scuticaria tigrina* and *Uropterygius macrocephalus* have a depressed ethmoid connection, whereas species *Enchelycore lichenosa*, *E. pardalis*, *E. schismatorhynchus*, *Gymnothorax albimarginatus*, *G. berndti*, *G. buroensis*, *G. fimbriatus*, *G. formosus*, *G. monochrous*, *G. intesi*, *G. kidako*, *G. margaritophorus*, *G. mucifer*, *G. neglectus*, *G. pictus*, *G. pseudothyrsoides*, *G. minor*, *G. thyrsoides*, and *G. ypsilon* were observed to have a dorsal margin that forms a straight line slanted towards the dorsal margin of the frontals (Fig. 20). Species of *Echidna*, *Strophidon*, *Gymnomuraena*, and some species of *Gymnothorax*, such as *G. chilospilus*, *G. eurostus*, *G. favagineus*, *G. flavimarginatus*, *G. leucostigma*, *G. meleagris*, *G. nudivomer*, *G. reevesii*, and *G. undulatus*, showed a small protrusion in between the premaxillary-ethmovomer and frontals (Fig. 21).

Some of the muraenids displayed either thin or wide anterodorsal part of the ethmoid. The character of having a flat and wide surface of ethmoid was observed in *Enchelycore lichenosa*, *Gymnothorax albimarginatus*, *G. pictus*, *G. reevesii*, and *G. undulatus*, whereas the rest of the specimens have a thin and long anterodorsal part of the ethmoid (Fig. 16). This character is unobservable in *Scuticaria tigrina* and *Uropterygius macrocephalus*. The posterior end of ethmoid also displayed characters of having either thin and short or wide and long surface. The species *Echidna nebulosa*, *Enchelycore lichenosa*, *E. schismatorhynchus*, *Gymnothorax albimarginatus*, *G. chilospilus*, *G. eurostus*,

G. favagineus, *G. fimbriatus*, *G. flavimarginatus*, *G. formosus*, *G. intesi*, *G. kidako*, *G. meleagris*, *G. nudivomer*, *G. pictus*, *G. pseudothyroideus*, *G. reevesii*, and *G. undulatus* were observed to have wide and long surface whereas the remaining species have thin and short posterior end of ethmoid.

The posterior end of the ethmoid displayed a groove for some of the species (Fig. 15). The character of the presence or absence of a shallow to deep pit is not uniform among *Gymnothorax* species. It was recorded from all of the specimens except in *Gymnomuraena zebra*, *Gymnothorax buroensis*, *G. favagineus*, *G. formosus*, *G. nudivomer*, *Scuticaria tigrina*, and *Uropterygius macrocephalus*. Another character in the joint between ethmoid and frontals is the recognizable small pore (Fig. 14). Similar to the groove, it is present mostly in *Gymnothorax* species except for *G. albimarginatus*, *G. berndti*, *G. fimbriatus*, *G. formosus*, *G. margaritophorus*, *G. thyroideus*, and *G. undulatus*. Similarly, the species under genus *Scuticaria*, *Strophidon*, and *Uropterygius* do not possess this character.



FIGURE 14. Pore in the joint of the ethmoid and frontals. A: absent; B: present.



FIGURE 15. Groove at the posterior end of the ethmoid. A: shallow; B: deep.

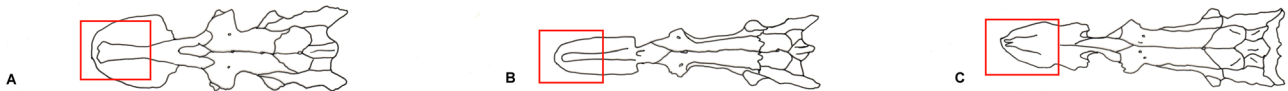


FIGURE 16. Surface of anterior part of ethmoid. A: flat and wide surface; B: thin and long; C: character is unobservable.



FIGURE 17. Surface of posterior end of ethmoid. A: thin; B: wide.



FIGURE 18. Shape of PEV plate from dorsal view. A: cone-shaped; B: round to oval-shaped.



FIGURE 19. Premaxilla size. A: short; B: long.



FIGURE 20. Lateral view of ethmoid. A: no depression; B: has depression.



FIGURE 21. The angle of ethmoid connection toward posterior end. A: angled position; B: has protrusion.



FIGURE 22. Proximal end of supraoccipital to pterotic. A: anterior; B: posterior.



FIGURE 23. Shape of supraoccipital crest. A: sharp; B: flattened.



FIGURE 24. Projection of supraoccipital median crest. A: greatly reduced; B: ascend outward.

The posterior ventral part of the PEV is the vomer. The vomerine processes consist of either short or long canine teeth which may also be recurved for all samples except for *Echidna nebulosa*, *E. polyzona*, and *Gymnomuraena zebra* that displays short and stout vomerine teeth (Fig. 25). The shape was characterized by these species as a special feature whereas *Gymnothorax nudivomer* renders the character unobservable.

The orbital region comprises the frontals, parasphenoid, pterosphenoids, sphenoids, and parietals. The frontals were not fused and bear a ridge at the midline (Fig. 27). The paired frontal expands laterally and its ventral part borders the orbit. This also serves as the roof of the cranium. A frontal connection site that has a protruding ridge was not observed in some species, e.g., *Echidna nebulosa*, *Gymnothorax albimarginatus*, *G. berndti*, *G. chilospilus*, *G. eurostus*, *G. flavimarginatus*, *G. intesi*, *G. leucostigma*, *G. margaritophorus*, *G. neglectus*, *G. nudivomer*, *G. pictus*, *G. reevesii*, *G. minor*, *G. thyrsoides*, *G. ypsilon*, *Scuticaria tigrina*, and *Uropterygius macrocephalus*.

The well-developed optic foramen is situated between the basisphenoid and the frontals. The pterosphenoid articulates with the basisphenoid, parasphenoid, sphenotic, pterotic, and frontal. It connects to the lateral part of the post-orbital region of the neurocranium. The parasphenoid, which is connected to the basisphenoid, is a long shaft of bone that extends from the posterior end of vomer to the basioccipital. It is expanded and conjoined with the remainder of the neurocranium, forming the floor of the braincase. The lateral side of parasphenoid consists of a paired short protruding process toward PEV (Fig. 28). It can be observed in *Gymnothorax favagineus*, *G. fimbriatus*, *G. formosus*, and *G. undulatus*.

Superior to parasphenoid is the basisphenoid. The unpaired basisphenoid has a process that barely extends into the orbit. This median vertical bone is compressed and the dorsal portion is elongated and guards the opening to the brain chamber. A small sharp process can be seen protruding from the basisphenoid of some species including *Echidna nebulosa*, *E. polyzona*, *Enchelycore lichenosa*, *E. pardalis*, *E. schismatorhynchus*, *Gymnothorax albimarginatus*, *G. berndti*, *G. flavimarginatus*, *G. favagineus*, *G. formosus*, *G. intesi*, *G. kidako*, *G. leucostigma*, *G. meleagris*, *G. minor*, *G. monochrous*, *G. mucifer*, *G. neglectus*, *G. nudivomer*, *G. pictus*, *G. pseudothyrsoides*, *G. undulatus*, and *G. ypsilon* (Fig. 26).

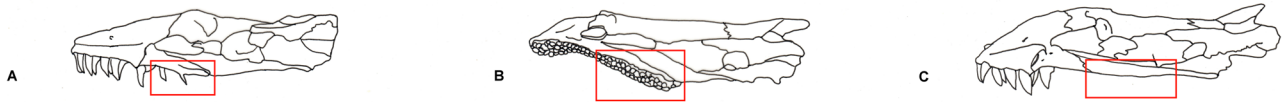


FIGURE 25. Vomerine teeth type. A: long and sharp; B: short and stout; C: character is unobservable



FIGURE 26. Extended sharp process at the basisphenoid. A: absent; B: present.



FIGURE 27. Ridge in the joint between frontals. A: absent; B: present.

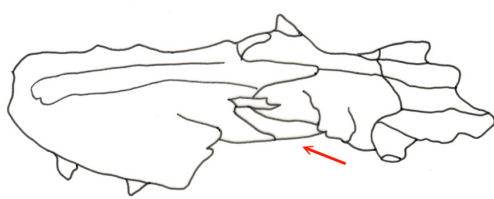
The occipital region is composed of the basioccipital, exoccipital and supraoccipital. The basioccipital is a large median bone forming the posterior part of the ventral side of the neurocranium. It is anteriorly attached to parasphenoid, anteroventral with the exoccipital and posteriorly drawn out into a keel-like structure for attachments of muscles on the neurocranium. Posteriorly, the basioccipital is expressed into an occipital condyle attached to the vertebral centrum, which possesses an opening (foramen) for blood vessels.

The exoccipitals are paired bones lying posterior to the supraoccipital and epiotics. Each exoccipital consists of a ventral flattened basal plate which meets its counterpart at the mid-ventral line to form the floor of the neurocranium. Also, the exoccipitals ventrally connects to the basioccipital and the posterior margin enclose the foramen magnum whose ventral rim is formed by the ventral basal plate. This bone takes part in the formation of foramen magnum for all of the species of moray eel.

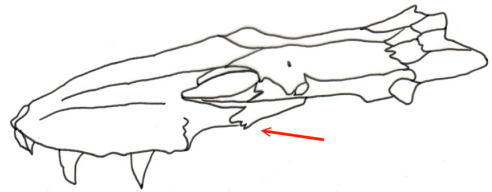
The epiotics form the posterodorsal face of the neurocranium. It is medially connected to the supraoccipital and exoccipital, and their anterior parts contact the pterotic and parietals. Dorsally, it displays either straight line and/or shallow curve or deep and pointed curve at the posterior margin of the neurocranium (Fig. 30). The species observed to have deep and pointed curve were *Gymnomuraena zebra*, *Gymnothorax berndti*, *G. fimbriatus*, *G. flavimarginatus*, *G. intesi*, *G. leucostigma*, *G. meleagris*, *G. neglectus*, *G. nudivomer*, *G. thyrsoideus*, and *G. undulatus*, whereas the remaining specimens have aligned or shallow curved margin.

The supraoccipital is a median bone located on the posterior extremity of the neurocranium. It articulates with the parietals anteriorly, the epiotics laterally, and the exoccipital posteriorly. Posterodorsally, the bone bears a ridge on which attaches the fascia between the two halves of the adductor mandibulae muscle. From the dorsal view of the neurocranium, the length of crest displayed on the supraoccipital is significant in *Gymnomuraena zebra* (Fig. 22). This character was absent in *Enchelycore schismatorhynchus*. Instead, it has a stout supraoccipital not exceeding the length of the pterotic. Other specimens that have a longer supraoccipital than pterotic include *Echidna polyzona*, *Gymnothorax flavimarginatus*, *G. intesi*, *G. leucostigma*, *G. nudivomer*, *G. pictus*, and *G. thyrsoideus*. On the lateral side of each neurocranium, the supraoccipital was observed to have either a well-developed or short and stout crest. The species *Echidna nebulosa*, *E. polyzona*, *Gymnomuraena zebra*, *Gymnothorax berndti*, *G. favagineus*, *G. intesi*, *G. monochrous*, *G. nudivomer*, *G. thyrsoideus*, and *Uropterygius macrocephalus* have a well-developed crest whereas the remaining specimen have a short and stout supraoccipital. Furthermore, the supraoccipital was characterized for having an ascending outward projection of the median crest in all specimens except for *Enchelycore pardalis* and *Gymnothorax albimarginatus*, that displayed a greatly reduced supraoccipital crest.

Lastly, the neurocranium of all examined species has a cream or pastel yellow coloration, except for *Echidna polyzona*, *Gymnomuraena zebra*, and *Gymnothorax thyrsoideus*, which have a light purple coloration. Moreover, the neurocranium of *Gymnothorax reevesii* has a pitted PEV surface, whereas larger samples have a dark pitted background. However, these do not penetrate to the ventral side of the vomer.

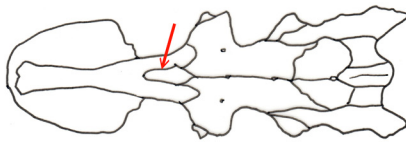


A

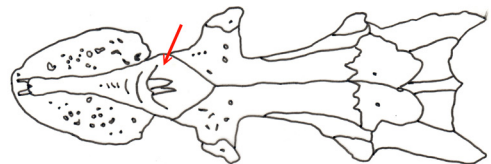


B

FIGURE 28. Extended process in the parasphenoid grown toward PEV. A: absent; B: present.

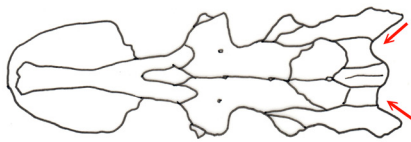


A

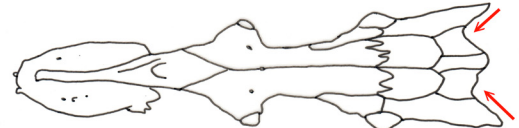


B

FIGURE 29. Outgrown process in the groove of the ethmoid. A: absent; B: present

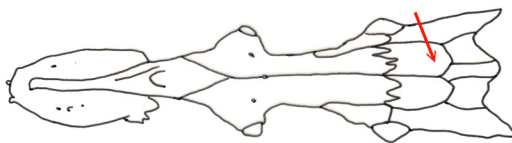


A

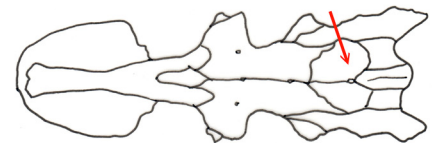


B

FIGURE 30. Curve at the posterior margin of exoccipital. A: shallow; B: deep and pointed.

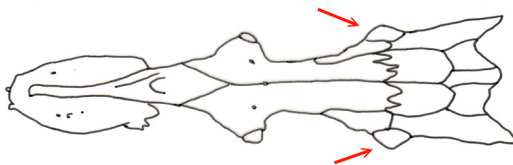


A

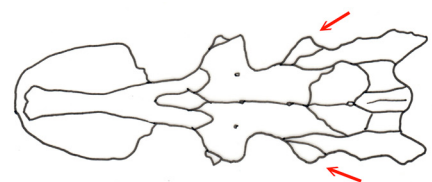


B

FIGURE 31. Pore at the anterior end of supraoccipital near parietal. A: absent or greatly reduced; B: well developed.



A



B

FIGURE 32. Sphenotic spine. A: no distal expansion; B: extended lateral process.

Discussion

The length measurements of neurocranial elements (Table 1) and the comparison of 20 morphological characters

indicate that neurocranium morphology differs among species, and each species can be identified by its features, although the degree of interspecific differentiation varies to some extent. Intraspecific differences in most neurocranium characters can be detected among species, except for the shape of paired frontals and lateral expansion of PEV plate which are stable characters within species, and even within genera. However, regarding other characters used in morphology-based taxonomy between Muraeninae and Uropterygiinae, the present results agreed with most of the previous conclusions that there is a distinction between the two subfamilies. Previous studies stated the differences in the fins, the subfamily Muraeninae having dorsal fin origin before or near gill opening, anal fin origin just behind anus; and the subfamily Uropterygiinae having dorsal and anal fin origin restricted to tail tip (McCosker & Smith, 1997; Böhlke & Randall, 2000; Böhlke & McCosker, 2001; Tang & Fielitz, 2013). The distinction between the two subfamilies is comparable to this study but herein using the relative ratio of the neurocranium to the depth of mid pre-orbit and orbit length as key to the subfamilies, the subfamily Uropterygiinae showed the highest value as compared to the subfamily Muraeninae. Species of Uropterygiinae have the lowest measurement on the orbit length and depth of pre-orbit due to the termination of the ethmoidal crest toward premaxilla. The swollen nasal cavity was observed in *Uropterygius macrocephalus* (Loh *et al.*, 2008), which may be formed by an accumulation of muscles on the depressed part of the ethmoidal crest. This is the first study to record the difference between the two subfamilies based on neurocranium osteology. However, these preliminary findings still need examination of more uropterygiine species to support this current conclusion.

The osteological study of muraenid eels illustrates the neurocranium characters present in members of this family. This is considered as the basis for future comparison as it is the first study to evaluate the neurocranium of moray eel species taken from Taiwanese waters. Based on observations of the neurocranium, *Gymnomuraena* was distinct from the genus *Echidna*, differing in the extended length of the supraoccipital process, slightly compressed skull, shorter premaxilla length, and shorter orbit length, although there are similarities in having molariform teeth and coloration, which may be a result of feeding on shellfish and crustaceans (Böhlke & Randall, 2000). The species of *Gymnomuraena* and *Echidna* were previously regarded as a monophyletic group due to several characters shared among durophagous morays (Mehta, 2009). However, Reece *et al.* (2010), demonstrated that durophagous feeding habits and associated morphological characters have evolved in parallel in *Gymnomuraena* and at least three additional times within the genus *Echidna*. This rejects the monophyly of the two genera indicating that the durophagous characters are not homologous.

In this study, it was observed that all species have vomerine teeth except *Gymnothorax nudivomer*. This species lacks of vomerine teeth in large adults (Smith *et al.*, 2008). Vomerine teeth in a single short series may be visible in smaller individuals of this species (Smith *et al.*, 2019).

Interestingly, a unique character was observed on the PEV plate of *Gymnothorax reevesii*, the pitted surface of PEV with dark background (Fig. 10C), where the pores did not penetrate through the ventral part. Previous studies by Chen *et al.* (1994), did not discuss this as it was not visible or had no connection to the external morphology of the species. For the supraoccipital, almost all species bear a crest on the supraoccipital, except for *Enchelycore schismatorhynchus* and *Gymnomuraena zebra*. The former having a reduced supraoccipital crest and the latter having significantly high supraoccipital. The neurocranium of *G. zebra* revealed a pronounced posteriorly directed supraoccipital which provides a greater surface area for attachment of muscles (Mehta, 2009). Relative ratios were highest mostly in *Gymnomuraena zebra* due to its posterior prolongation and shortest measurements on ethmoid, pre-orbit, orbit, PEV, and frontal width. Lowest values were recorded in *Gymnothorax albimarginatus*, *G. flavimarginatus*, *G. formosus*, *G. minor*, *G. pictus*, *Enchelycore schismatorhynchus*, and *E. lichenosa*.

One species of *Gymnothorax* distributed in Taiwanese waters has been previously synonymized with *Gymnothorax kidako* (Böhlke & Randall, 2000). However, recent morphological study on the body color pattern and meristic characters of the species show they do not conform to the general condition of *G. kidako* in Japan and Taiwan. It was then reevaluated and distinguished as *Gymnothorax mucifer* based on morphological and molecular data (Huang *et al.*, 2019). This distinction supports the differences on morphometric and morphological characters of *G. kidako* in having a wider and long ethmoid surface compared to *G. mucifer*.

Conclusion

Osteological characters play a very important role in the classification of different species. The neurocranium of 34

muraenid species were examined, described, and figured to evaluate the family Muraenidae. These data can serve as a basis for future investigation of cranial morphometrics in morays. Based on this study, some important characters, specifically on the neurocranium, differentiated muraenid species. There is a need for further study and inclusion of more characters from other skeletal parts to differentiate these species. Future phylogenetic studies on morays will greatly contribute to understanding the morphological diversity underlying this family.

Acknowledgements

We appreciated the anonymous reviewers and very grateful to Dr. David G. Smith in giving invaluable comments on the manuscript. We also thank the colleagues in the Laboratory of Aquatic Ecology, National Taiwan Ocean University, for their assistance in specimen collection.

References

- Abbott, C.C. (1860) Description of new species of apodal fishes in the museum of the Academy of Natural Sciences of Philadelphia. *Proceedings of the Academy of Natural Sciences of Philadelphia*, 12, 475–479.
- Ahl, J.N. (1789) *Specimen ichthyologicum de Muraena et Ophichtho, quod venia exp. fac. med. ups. Praeside Carol. Pet. Thunberg, etc.* J. Edman, Uppsala, 14 pp.
- Bennett, E.T. (1832) Observations on a collection of fishes from the Mauritius, presented by Mr. Telfair, with characters of new genera and species. *Proceedings of the Committee of Science and Correspondence of the Zoological Society of London*, 1830–1831 (1), 165–169.
- Bleeker, P. (1853) Derde bijdrage tot de kennis der ichthyologische fauna van Celebes. *Natuurkundig Tijdschrift voor Nederlandsch Indië*, 3 (5), 739–782.
- Bleeker, P. (1856) Zevende bijdrage tot de kennis der ichthyologische fauna van Ternate. *Natuurkundig Tijdschrift voor Nederlandsch Indië*, 10, 357–386.
- Bleeker, P. (1857) Tweede bijdrage tot de kennis der ichthyologische fauna van Boero. *Natuurkundig Tijdschrift voor Nederlandsch Indië*, 13 (1), 55–82.
- Bleeker, P. (1864) Poissons inédits indo-archipélagiques de l'ordre des Murènes. *Nederlandsch Tijdschrift voor de Dierkunde*, 2, 38–54.
- Bloch, M.E. & Schneider, J.G. (1801) *Systema ichthyologiae iconibus cx illustratum. Post obitum auctoris opus inchoatum absolvit, correxit, interpolavit Jo. Gottlob Schneider, Saxo.* Sanderiano, Berlin, 584 pp.
<https://doi.org/10.5962/bhl.title.5750>
- Böhlke E.B. & McCosker J.E. (2001) The moray eels of Australia and New Zealand, with the description of two new species (Anguilliformes: Muraenidae). *Records of the Australian Museum*, 53, 71–102.
<https://doi.org/10.3853/j.0067-1975.53.2001.1325>
- Böhlke, E.B., McCosker, J.E. & Böhlke, J.E. (1989) Family Muraenidae. In: Böhlke, E.B. (Ed.), *Fishes of the Western North Atlantic. Memoirs of the Sears Foundation for Marine Research. 1 (Part 9)*. Sears Foundation for Marine Research, New Haven, pp. 104–206.
- Böhlke, E.B. & Randall, J.E. (2000) A review of the moray eels (Anguilliformes: Muraenidae) of the Hawaiian Islands, with descriptions of two new species. *Proceedings of the Academy of Natural Sciences of Philadelphia*, 150, 203–278.
- Chen, H.-M., Shao, K.-T. & Chen, C.-T. (1994) A review of the muraenid eels (family Muraenidae) from Taiwan with descriptions of twelve new records. *Zoological Studies*, 33 (1), 44–64.
- Collar, D.C., Reece, J.S., Alfaro, M.E., Wainwright, P.C. & Mehta, R.S. (2014) Imperfect morphological convergence: variable changes in cranial structures underlie transitions to durophagy in moray eels. *The American Naturalist*, 183 (6), E168–E184.
<https://doi.org/10.1086/675810>
- Eagderi, S. & Adriaens, D. (2014) Cephalic morphology of *Ariosoma gilberti* (Bathymyrinae: Congridae). *Iranian Journal of Ichthyology*, 1 (1), 39–50.
- Fricke, R., Eschmeyer, W.N. & van der Laan, R. (Eds.) (2020) Eschmeyer's Catalog of Fishes: Genera, Species, References. Available from: <http://researcharchive.calacademy.org/research/ichthyology/catalog/fishcatmain.asp> (accessed 5 March 2020)
- Fielitz, C. (2002) Previously unreported pectoral bones in moray eels (Anguilliformes: Muraenidae). *Copeia*, 2002 (2), 483–488.
[https://doi.org/10.1643/0045-8511\(2002\)002\[0483:PUPBIM\]2.0.CO;2](https://doi.org/10.1643/0045-8511(2002)002[0483:PUPBIM]2.0.CO;2)
- Fourmanoir, P. & Rivaton, J. (1979) Poissons de la pente récifale externe de Nouvelle-Calédonie et des Nouvelles-Hébrides. *Cahiers de l'Indo-Pacifique*, 1 (4), 405–443.
- Hamilton, F. (1822) *An Account of the Fishes Found in the River Ganges and Its Branches*. Archibald Constable and Company,

Edinburgh, 405 pp.

- Hatooka, K. & Randall, J.E. (1992) A new moray eel (*Gymnothorax*: Muraenidae) from Japan and Hawaii. *Japanese Journal of Ichthyology*, 39 (3), 183–190.
<https://doi.org/10.11369/jji1950.39.183>
- Huang, W.-C., Chen, H.-M. & Liao, T.-Y. (2019) Revalidation of a moray eel, *Gymnothorax mucifer* Snyder, 1904 (Teleostei: Anguilliformes: Muraenidae), with a revised distribution. *Zootaxa*, 4559 (1), 151–165.
<https://doi.org/10.11646/zootaxa.4559.1.6>
- Jordan, D.S & Richardson, R.E. (1909) A catalogue of the fishes of the island of Formosa, or Taiwan, based on the collections of Dr. Hans Sauter. *Memoirs of the Carnegie Museum*, 4 (4), 159–204.
- Jordan, D.S. & Snyder, J.O. (1901) A review of the apodal fishes or eels of Japan, with descriptions of nineteen new species. *Proceedings of the United States National Museum*, 23 (1239), 837–890.
<https://doi.org/10.5479/si.00963801.23-1239.837>
- Lacepède, B.G.E. (1803) *Histoire naturelle des poissons. Vol. 5*. Chez Plassan, Paris, 803 pp.
<https://doi.org/10.5962/bhl.title.6882>
- Lesson, R.P. (1828) Description du nouveau genre *Ichthyophis* et de plusieurs espèces inédites ou peu connues de poissons, recueillis dans le voyage autour du monde de la corvette *La Coquille*. *Mémoires de la Société d'Histoire Naturelle Paris, Série 2*, 4, 397–412.
- Loh, K.-H., Chen, I.-S., Randall, J.E. & Chen, H.-M. (2008) A review and molecular phylogeny of the moray eel subfamily Uropterygiinae (Anguilliformes: Muraenidae) from Taiwan, with description of a new species. *The Raffles Bulletin of Zoology*, 19, 135–150.
- Loh, K.-H., Shao, K.-T. & Chen, H.-M. (2011) *Gymnothorax melanosomatus*, a new moray eel (Teleostei: Anguilliformes: Muraenidae) from southeastern Taiwan. *Zootaxa*, 3134 (1), 43–52.
<https://doi.org/10.11646/zootaxa.3134.1.2>
- Mehta, R.S. (2009) Ecomorphology of the moray bite: relationship between dietary extremes and morphological diversity. *Physiological and Biochemical Zoology*, 82 (1), 90–103.
<https://doi.org/10.1086/594381>
- Mehta, R.S. & Wainwright, P.C. (2007) Raptorial jaws in the throat help moray eels swallow large prey. *Nature*, 449, 79–82.
<https://doi.org/10.1038/nature06062>
- McCosker, J.E. & Smith, D.G. (1997) Two new Indo-Pacific morays of the genus *Uropterygius* (Anguilliformes: Muraenidae). *Bulletin of Marine Science*, 60 (3), 1005–1014.
- Playfair, R.L. & Günther, A.C.L.G. (1867) *The Fishes of Zanzibar*. John Van Voorst, London, 153 pp.
<https://doi.org/10.5962/bhl.title.6900>
- Reece, J.S., Bowen, B.W., Smith, D.G. & Larson, A.F. (2010) Molecular phylogenetics of moray eels (Muraenidae) demonstrates multiple origins of shell-crushing jaw (*Gymnomuraena*, *Echidna*) and multiple colonizations of the Atlantic Ocean. *Molecular Phylogenetics and Evolution*, 57, 829–835.
<https://doi.org/10.1016/j.ympev.2010.07.013>
- Richardson, J. (1845a) Ichthyology. Part 2. In: Hinds, R.B. (Ed.), *The Zoology of the Voyage of H.M.S. Sulphur, under the Command of Captain Sir Edward Belcher, R.N., C.B., F.R.G.S., etc., during the Years 1836–42. Vol. 1*. Smith, Elder and Co., London, pp. 71–98.
- Richardson, J. (1845b) Ichthyology. Part 3. In: Hinds, R.B. (Ed.), *The Zoology of the Voyage of H.M.S. Sulphur, under the Command of Captain Sir Edward Belcher, R.N., C.B., F.R.G.S., etc., during the Years 1836–42. Vol. 1*. Smith, Elder and Co., London, pp. 99–150.
- Rüppell, E. (1830) *Atlas zu der Reise im nördlichen Afrika. Fische des rothen Meers*. Heinr. Lud, Brönnner, Frankfurt am Main, 144 pp.
<https://doi.org/10.5962/bhl.title.53779>
- Shao, K.-T., Ho, H.-C., Lin, P.-L., Lee, P.-F., Lee, M.-Y., Tsai, C.-Y., Liao, Y.-C., Lin, Y.-C., Chen, J.-P. & Yeh, H.-M. (2008) A checklist of the fishes of southern Taiwan, northern South China Sea. *The Raffles Bulletin of Zoology*, Supplement 19, 233–271.
- Shaw, G. & Nodder, F.P. (1795) *The Naturalist's Miscellany: or, Coloured Figures of Natural Objects; Drawn and Described from Nature. Vol. 7*. Nodder & Co., London. [unnumbered pages]
<https://doi.org/10.5962/bhl.title.79941>
- Shaw, G. & Nodder, F.P. (1797) *The Naturalist's Miscellany: or, Coloured Figures of Natural Objects; Drawn and Described from Nature. Vol. 9*. Nodder & Co., London. [unnumbered pages]
<https://doi.org/10.5962/bhl.title.79941>
- Smith, D.G. (2012) A checklist of the moray eels of the world (Teleostei: Anguilliformes: Muraenidae). *Zootaxa*, 3474 (1), 1–64.
<https://doi.org/10.11646/zootaxa.3474.1.1>
- Smith, D.G. & Böhlke, E.B. (1997) A review of the Indo-Pacific banded morays of the *Gymnothorax reticularis* group, with descriptions of three new species (Pisces, Anguilliformes, Muraenidae). *Proceedings of the Academy of Natural Sciences of Philadelphia*, 148, 177–188.
- Smith, D.G., Brokovich, E. & Einbinder, S. (2008) *Gymnothorax baranesi*, a new moray eel (Anguilliformes: Muraenidae) from

- the Red Sea. *Zootaxa*, 1678 (1), 63–68.
<https://doi.org/10.11646/zootaxa.1678.1.4>
- Smith D.G., Bogorodsky, S.V., Mal, A.O. & Alpermann, T.J. (2019) Review of the moray eels (Anguilliformes: Muraenidae) of the Red Sea, with description of a new species. *Zootaxa*, 4704 (1), 1–87.
<https://doi.org/10.11646/zootaxa.4704.1.1>
- Snyder, J.O. (1904) A catalogue of the shore fishes collected by the steamer Albatross about the Hawaiian Islands in 1902. *Bulletin of the United States Fish Commission*, 22, 513–538.
- Tanaka, S. (1911) *Figures and Descriptions of the Fishes of Japan, including Riukiu Islands, Bonin Islands, Formosa, Kurile Islands, Korea and southern Sakhalin. Vol. 2.* Tokyo Printing Co., Tokyo, pp. 19–34.
<https://doi.org/10.5962/bhl.title.13715>
- Tang, K.L. & Fielitz, C. (2013) Phylogeny of moray eels (Anguilliformes: Muraenidae), with a revised classification of true eels (Teleostei: Elopomorpha: Anguilliformes). *Mitochondrial DNA*, 24 (1), 55–66.
<https://doi.org/10.3109/19401736.2012.710226>
- Temminck, C.J. & Schlegel, H. (1846) Pisces. In: Siebold, P.F. de (Ed.), *Fauna Japonica, sive descriptio animalium, quae in itinere per Japoniam, jussu et auspiciis, superiorum, qui summum in India Batava imperium tenent, suscepto, annis 1823–1830 collegit, notis, observationibus et adumbrationibus illustravit Ph. Fr. de Siebold. Parts 10–14.* Apud Arnz et Socios, Leiden, pp. 173–269.
<https://doi.org/10.5962/bhl.title.124951>